Electronic Supplementary Material (ESI) for Journal of Materials Chemistry C.
This journal is © The Royal Society of Chemistry 2023

Supporting Information

for

Homoleptic purine-based NHC iridium(III) complexes for blue OLED application: impact of isomerism on photophysical properties

Armands Sebris,[a] Matas Guzauskas,[b] Malek Mahmoudi,[b] Dmytro Volyniuk,[b] Juozas V. Grazulevicius,[b] Anatoly Mishnev,[c] Irina Novosjolova,[a] Māris Turks,[a] Gediminas Jonusauskas,[d] Kaspars Traskovskis [e*]

[a] *Institute of Technology of Organic Chemistry, Faculty of Materials Science and Applied Chemistry, Riga Technical University, P. Valdena Str. 3, LV-1048, Riga, Latvia*

[b] *Department of Polymer Chemistry and Technology, Kaunas University of Technology, Barsausko 59, LT- 51423, Kaunas, Lithuania*

[c] *Latvian Institute of Organic Synthesis, Aizkraukles Str. 21, Riga, LV-1006, Latvia*

[d] *Laboratoire Ondes et Matière d'Aquitaine, Bordeaux University, UMR CNRS 5798, 351 Cours de la Libération, 33405 Talence, France*

[e] *Institute of Applied Chemistry, Faculty of Materials Science and Applied Chemistry, Riga Technical University, P. Valdena Str. 3, LV-1048, Riga, Latvia, e-mail: kaspars.traskovskis@rtu.lv*

Table of Contents

1. Experimental procedures S3
1.1. Synthesis.....S3
1.2. Thermal properties S12
1.3. Photophysical characterizations S12
1.4. Fabrication and characterization of PhOLEDs.....S13
1.5. Photoelectron emission spectroscopy.....S13
1.6. DFT calculations S14
X-ray analysis S15
Thermal properties S17
Figure S1. .....S17
Table S3.....S17
Table S4.....S17
Temperature dependent PL measurements in doped polymer films.....S18
Figure S2. .....S19
Figure S3. .....S20
Photophysical properties.....S20
Table S5.....S20
Figure S4. .....S21
Table S6.....S21
DFT Calculations.....S22
Table S7.....S22
Figure S5. .....S23
Table S8.....S23
Electrical and electroluminescent properties S24
Figure S6. .....S24
Figure S7. .....S24
Figure S8. .....S25
Figure S9. .....S25
Figure S10. .....S26
Figure S11. .....S26
Table S9.....S27
DFT optimized molecular geometries S28
References.....S34

1. Experimental procedures

1.1. Synthesis

General procedures. Commercial reagents (Acros, Alfa Aesar, Fluorochem, BLD Pharm) were used as received. Reactions and purity of the synthesized compounds were monitored by TLC using silica gel 60 F254 aluminum plates precoated with a 0.25 mm layer of silica gel (Merck). Visualization was accomplished by UV light. Column chromatography was performed using silica gel 60 (0.040–0.063 mm) (Upasil). Yields refer to chromatographically and spectroscopically homogeneous materials (with purity≥95%).

NMR spectra were recorded on Bruker Avance 500 spectrometers. ^{1}H NMR spectra were recorded at 500 MHz, with internal references from residual nondeuterated solvents (δ = 7.26 for $CDCl_3$ and δ = 2.50 for DMSO-d_6). ^{13}C NMR spectra were recorded at 125.7 MHz with internal references from solvent carbon signals (δ = 77.16 for $CDCl_3$ and δ = 39.52 for DMSO-d_6) with no internal reference. Coupling constants are reported in Hz and chemical shifts of signals are given in ppm and standard abbreviations were used for multiplicity assignments. The infrared spectra were recorded with an FTIR Perkin-Elmer Spectrum 100 spectrometer.

For HPLC analyses Agilent Technologies 1200 Series system was used (X Bridge C18 column, 4.6 × 150 mm, particle size 3.5 μm). Eluent A: 0.1% aq TFA/CH_3CN (95:5, v/v), eluent B: CH_3CN. Gradient: 30–95% B 5 min, 95% B 5 min, 95–30% B 2 min. Flow rate: 1 mL/min. Wavelength of detection was set to 260 nm.

HRMS analysis was performed on a Waters Synapt GII Q-ToF UPLC/MS system for compounds **1**-**6**, ***mer*-PhP** and Agilent 1290 Infinity series UPLC system connected to Agilent 6230 TOF LC/MS mass spectrometer for compound ***fac*-PhP**. Column Extend C18 RRHD 2.1 × 50 mm, 1.8 μm. Eluents: formic acid in CH_3CN (0.1%) and aq. 0.1% formic acid.

6-Chloro-*N*^{5}-methyl-*N*^{4}-phenylpyrimidine-4,5-diamine (3)

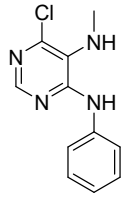

To a solution of compound **2** (3.0 g, 16.85 mmol, 1.0 eq.) in *i*-PrOH (30 mL) aniline (4.57 mL, ρ = 1.03 g/cm^3, 50.56 mmol, 3.0 eq.) was added and the reaction mixture was stirred for 40 h at 70 °C. The reaction mixture was then evaporated and silica gel column chromatography (Tol/MeCN, gradient 0% → 10%) provided product **3** (yield: 3.15 g, 80%) as a colourless solid. R_f = 0.40 (Tol/MeCN = 10:1). HPLC: t_R = 4.66 min. IR (KBr) ν (cm^{-1}): 3302, 3249, 2947, 1596, 1559, 1508, 1446, 1400, 1224. ^{1}H-NMR (500 MHz, $CDCl_3$) δ (ppm): 8.29 (s, 1H, H-C(2)), 7.76–7.60 (br. s, 1H, H-N), 7.65 (d, 2H, ^3J = 7.6 Hz, 2×H-C(Ar)), 7.38 (t, 2H, ^3J = 7.6 Hz, 2×H-C(Ar)), 7.12 (t, 1H, ^3J = 7.6 Hz, H-C(Ar)), 3.10–2.98 (br. s, 1H, H-N), 2.74 (s, 3H, (-CH_3)). ^{13}C-NMR (126 MHz, $CDCl_3$) δ (ppm): 157.2, 153.5, 152.4, 138.5, 129.2, 125.4, 124.0, 120.6, 34.3. HRMS (ESI) m/z: $[M+H]^+$ Calcd for $C_{11}H_{12}ClN_4$ 235.0750; Found 235.0755.

^{1}H-NMR (500 MHz, $CDCl_3$) spectrum of compound 3:

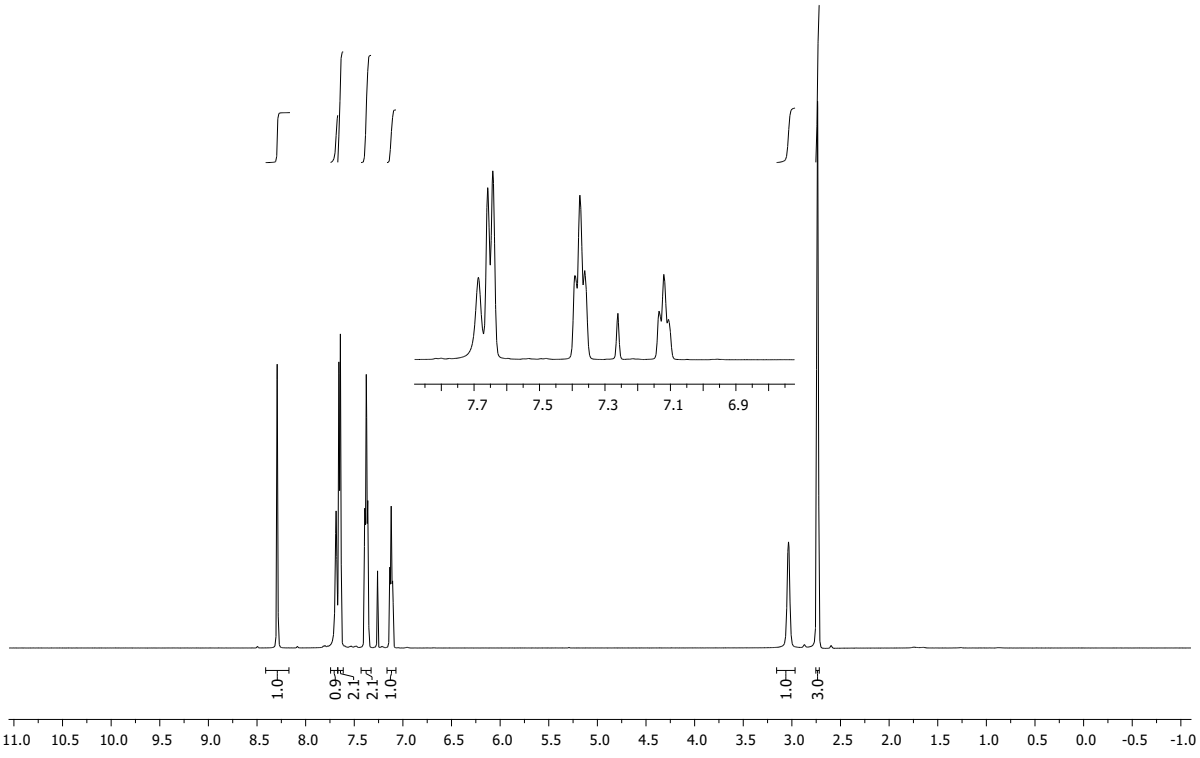

^{13}C-NMR (126 MHz, $CDCl_3$) spectrum of compound 3:

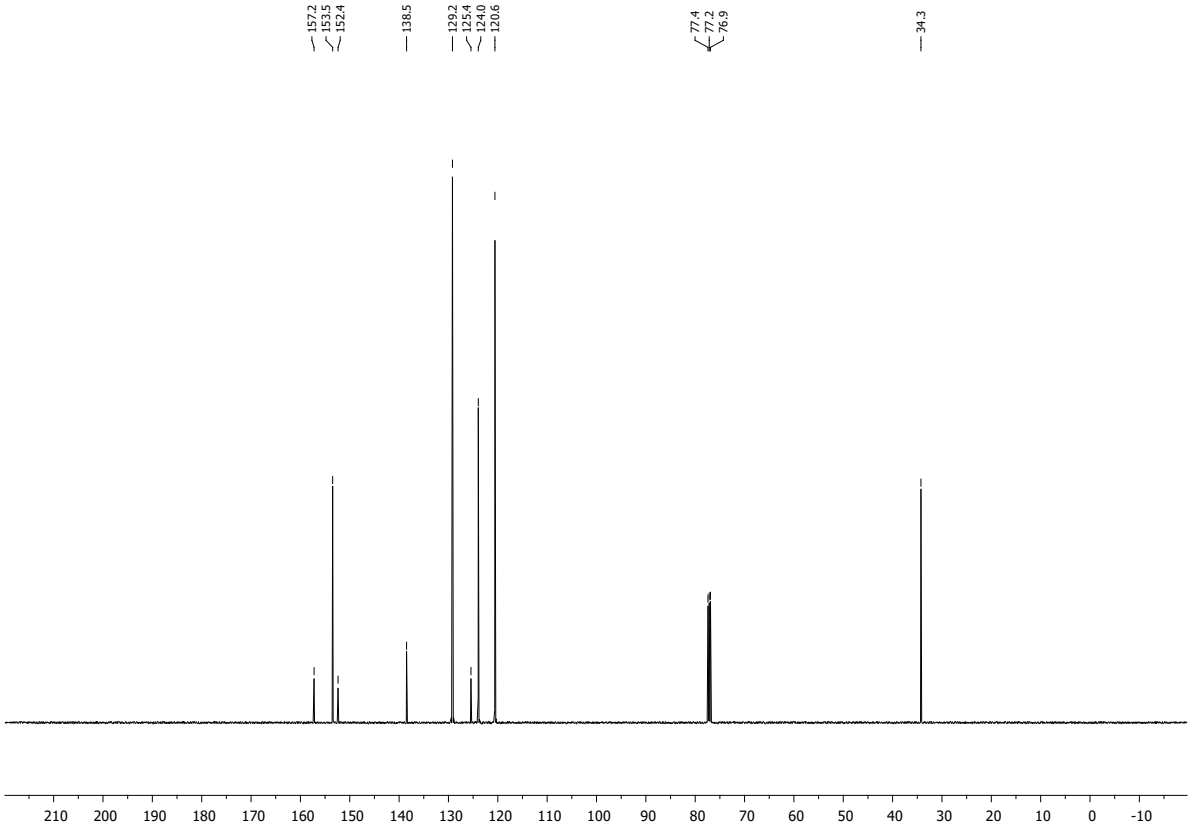

***N*^{5}-Methyl-*N*^{4}-phenylpyrimidine-4,5-diamine (4)**

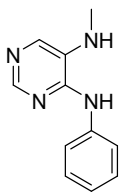

To a solution of compound **3** (1.5 g, 6.38 mmol, 1.0 eq.) in MeOH (100 mL), 10w% Pd/C (150 mg) and HCOOH (0.24 mL, ρ = 1.22 g/cm^3, 6.38 mmol, 1.0 eq.) were added and the reaction was stirred at 20 °C for 1 h, while H_2 was simultaneously bubbled through the suspension. Upon completion, the reaction mixture was filtered through celite and washed with MeOH (2 × 20 mL). The filtrate was evaporated and suspended in sat. aq. $NaHCO_3$ (50 mL). The aqueous suspension was extracted with DCM (6 × 100 mL), combined aqueous layers were washed with brine (50 mL), dried over anh. Na_2SO_4, filtered and evaporated to yield product **4** (yield: 1.20 g, 94%) as an off-white solid. R_f = 0.63 (DCM/EtOH = 10:1). HPLC: t_R = 2.25 min. IR (KBr) ν (cm^{-1}): 3345, 3295, 3036, 1603, 1575, 1497, 1440, 1410, 1234. ^{1}H-NMR (500 MHz, DMSO-d_6) δ (ppm): 8.34–8.28 (br. s, 1H, H-N), 8.06 (s, 1H, H-C(2)), 7.71 (d, 2H, ^3J = 7.6 Hz, 2×H-C(Ar)), 7.65 (s, 1H, H-C(6)), 7.31 (t, 2H, ^3J = 7.6 Hz, 2×H-C(Ar)), 7.00 (t, 1H, ^3J = 7.6 Hz, H-C(Ar)), 5.48–5.38 (br. s, 1H, H-N), 2.80 (s, 3H, (-CH_3)). ^{13}C-NMR (126 MHz, DMSO-d_6) δ (ppm): 148.7, 145.9, 140.1, 132.6, 129.9, 128.5, 122.1, 120.2, 29.4. HRMS (ESI) m/z: $[M+H]^+$ Calcd for $C_{11}H_{13}N_4$ 201.1135; Found 201.1130.

^{1}H-NMR (500 MHz, DMSO-d_6) spectrum of compound 4:

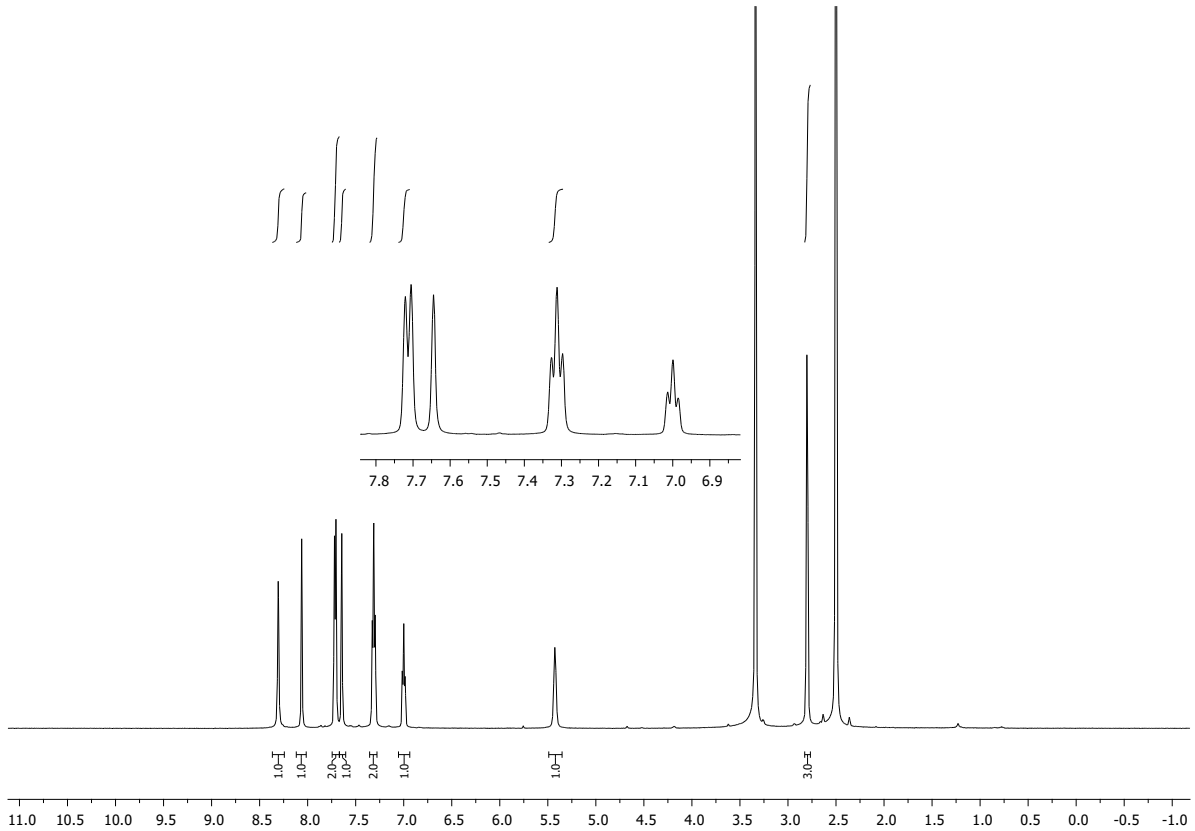

^{13}C-NMR (126 MHz, DMSO-d_6) spectrum of compound 4:

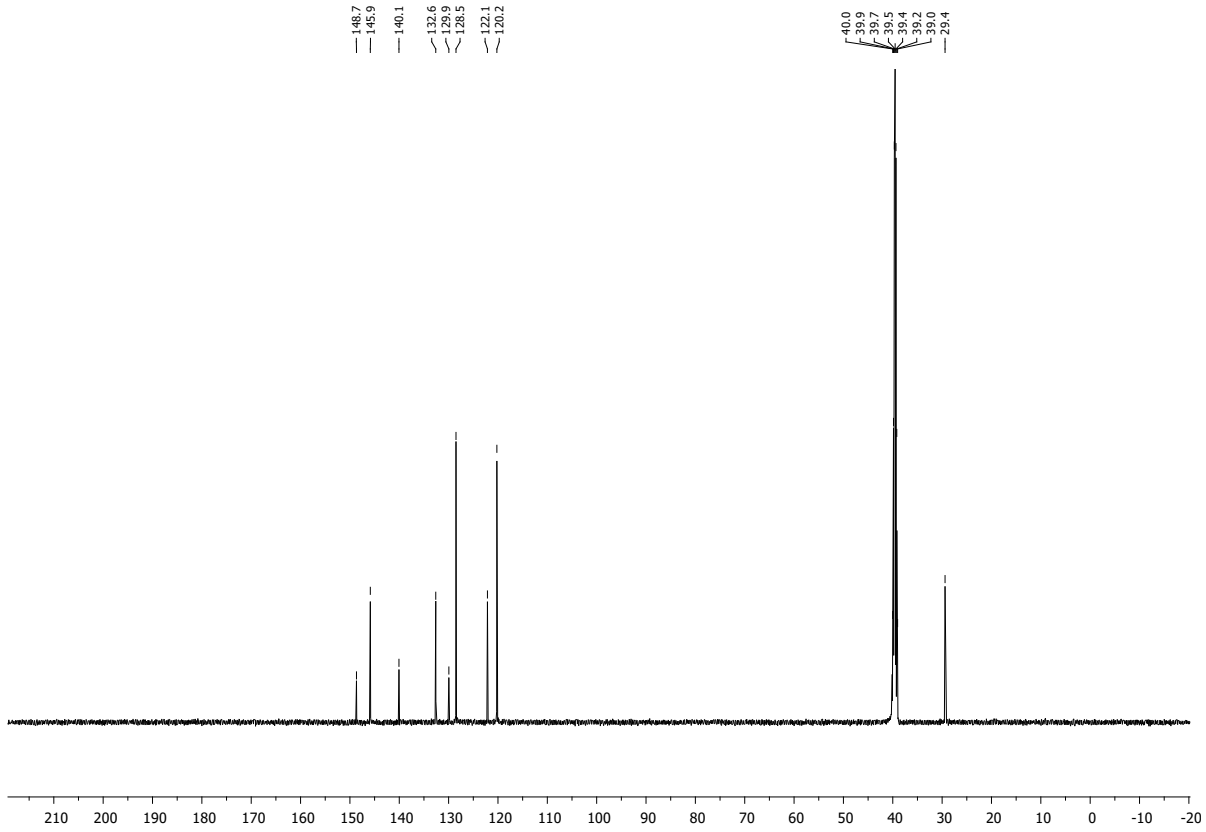

7-Methyl-9-phenyl-9*H*-purin-7-ium chloride (5)

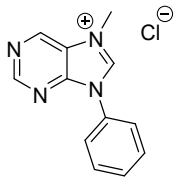

To a solution of compound **4** (1.5 g, 7.50 mmol, 1.0 eq.) in $HC(OEt)_3$ (60 mL), 4N HCl in dioxane (1.88 mL, 7.50 mmol, 1.0 eq.) and a drop of HCOOH was added and the reaction mixture was stirred at 60 ℃ for 2 h. Reaction mixture was allowed to cool to 20 ℃ and then was kept at -20 ℃ for 1 h. The suspension was then filtered and washed with EtOAc (2 × 10 mL) and the solids were dried overnight. Recrystallization from dry MeCN under argon yielded product **3** (yield: 1.17 g, 63%) as an off-white solid. R_f = 0.68 (DCM/EtOH = 10:1). HPLC: t_R = 1.96 min. IR (KBr) ν (cm^{-1}): 2971, 1682, 1645, 1605, 1563, 1460, 1242. ^{1}H-NMR (500 MHz, DMSO-d_6) δ (ppm): 10.76 (s, 1H, H-C(8)), 9.83 (s, 1H, H-C(6)), 9.41 (s, 1H, H-C(2)), 7.92 (d, 2H, ^3J = 7.5 Hz, 2×H-C(Ar)), 7.76 (t, 2H, ^3J = 7.5 Hz, 2×H-C(Ar)), 7.70 (t, 1H, ^3J = 7.5 Hz, H-C(Ar)), 4.30 (s, 3H, (-CH_3)). ^{13}C-NMR (126 MHz, DMSO-d_6) δ (ppm): 155.7, 148.0, 146.4, 145.9, 131.9, 130.4, 130.0, 124.9, 124.2, 34.6. HRMS (ESI) m/z: $[M+H]^+$ Calcd for $C_{12}H_{12}N_4$ 211.0984; Found 211.0991.

^{1}H-NMR (500 MHz, DMSO-d_6) spectrum of compound 5:

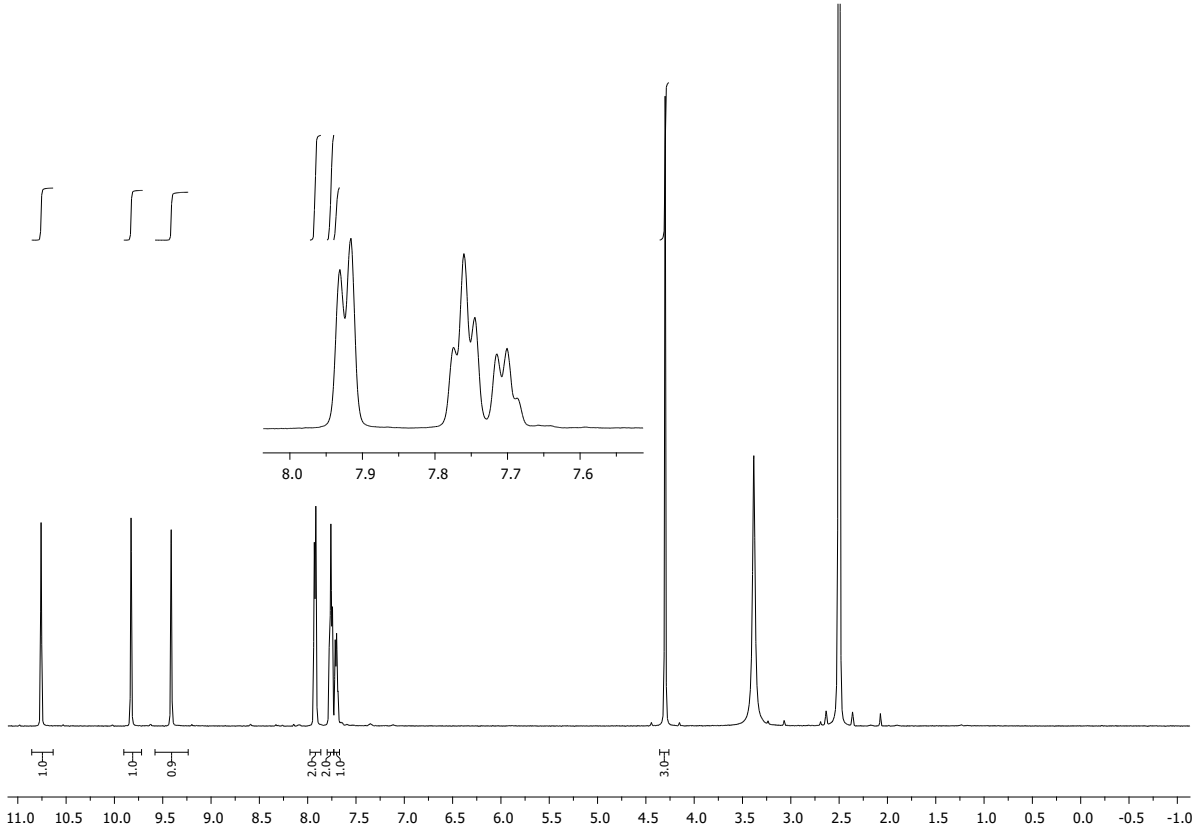

^{13}C-NMR (126 MHz, DMSO-d_6) spectrum of compound 5:

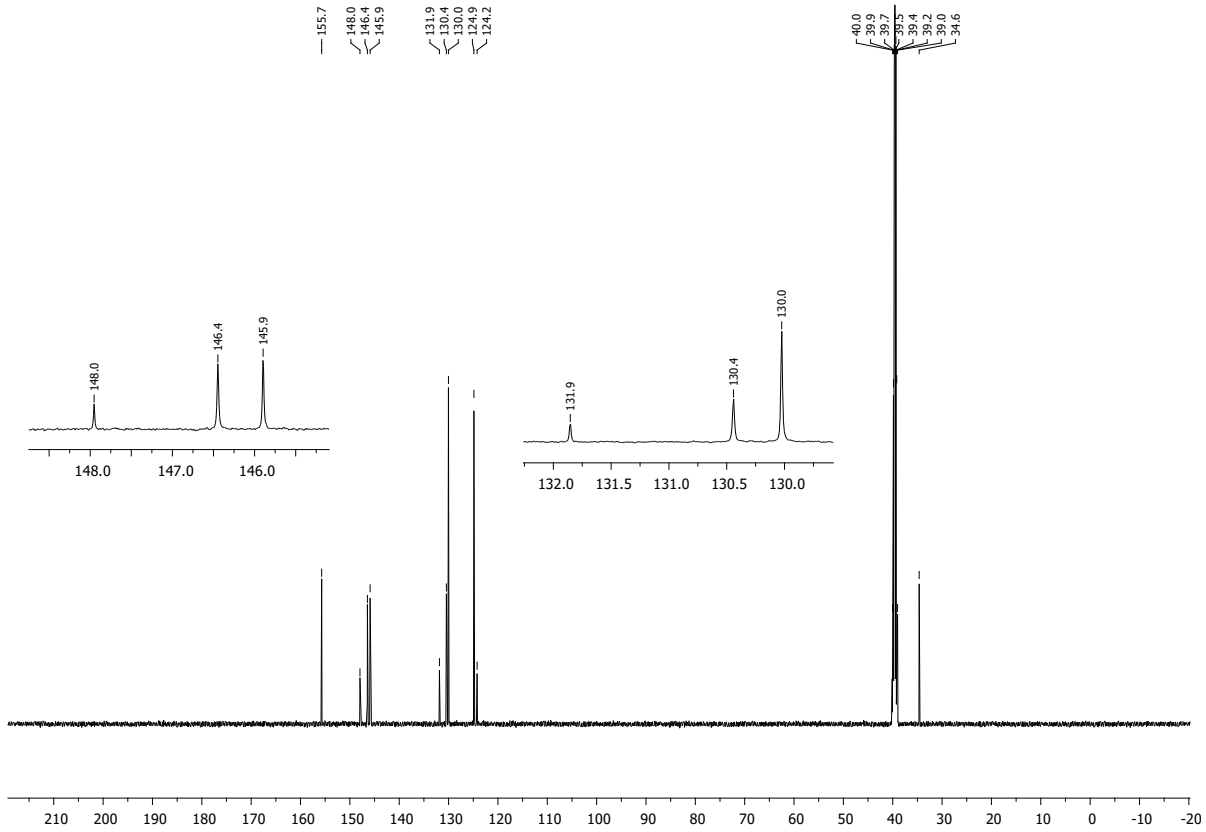

***Mer*-tris-(7-methyl-9-phenyl-purin-8-yl)iridium (*mer*-PhP)**

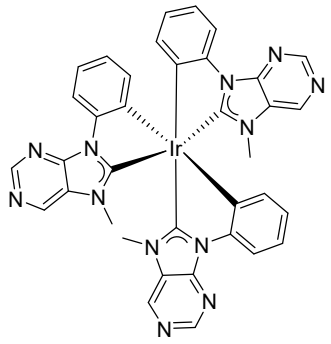

Compound **5** (494 mg, 2.00 mmol, 6.0 eq.), AgOAc (668 mg, 4.00 mmol, 12.0 eq.) and $[Ir(COD)Cl]_2$ (224 mg, 0.33 mmol, 1.0 eq.) were placed in a flask under septum and air was exchanged to argon at a Schlenk line. Degassed, dry PhCl (34 mL) was added and the reaction mixture was stirred at 80 °C for 16 h. Upon completion, solvent was evaporated and silica gel column chromatography (DCM/EtOH gradient 0% → 4%) provided product ***mer*-PhP** (yield: 365 mg, 67%) as a pale yellow solid. R_f = 0.73 (DCM/EtOH = 10:1). HPLC: t_R = 6.10 min. IR (KBr) ν (cm^{-1}): 3045, 1600, 1570, 1479, 1426, 1331, 1182. ^{1}H-NMR (500 MHz, $CDCl_3$) δ (ppm): 9.04, 9.04, 9.00 (3s, 3H, 3×H-C(2)), 8.78, 8.73, 8.69 (3d, 3H, ^3J = 7.9 Hz, 3×H-C(Ar)), 8.67, 8.64, 8.61 (3s, 3H, 3×H-C(6)), 7.09, 7.08, 7.03 (3t, 3H, ^3J = 7.8 Hz, 3×H-C(Ar)), 6.88, 6.84, 6.47 (3d, 3H, ^3J = 7.6 Hz, 3×H-C(Ar)), 6.81, 6.76, 6.73 (3t, 3H, ^3J = 7.2 Hz, 3×H-C(Ar)), 3.38, 3.33, 3.26 (3s, 9H, 3×(-CH_3)). ^{13}C-NMR (126 MHz, $CDCl_3$) δ (ppm): 193.2, 190.1, 189.0, 153.1, 153.0, 152.8, 150.5, 150.4 (2C),[1] 147.6, 147.1, 146.6, 145.5, 145.4, 143.3, 139.2, 138.7, 136.8, 136.5, 136.1, 135.8, 128.2 (2C), 127.9, 126.6, 126.5 ,126.4,

[1] Determined from HSQC and HMBC NMR spectra.

122.5, 122.0, 121.8, 116.0, 115.9, 115.4, 34.4, 34.3, 33.6. HRMS (ESI) m/z: $[M+H]^+$ Calcd for $C_{36}H_{28}N_{12}Ir$ 821.2189; Found 821.2203.

^{1}H-NMR (500 MHz, $CDCl_3$) spectrum of compound *mer*-PhP:

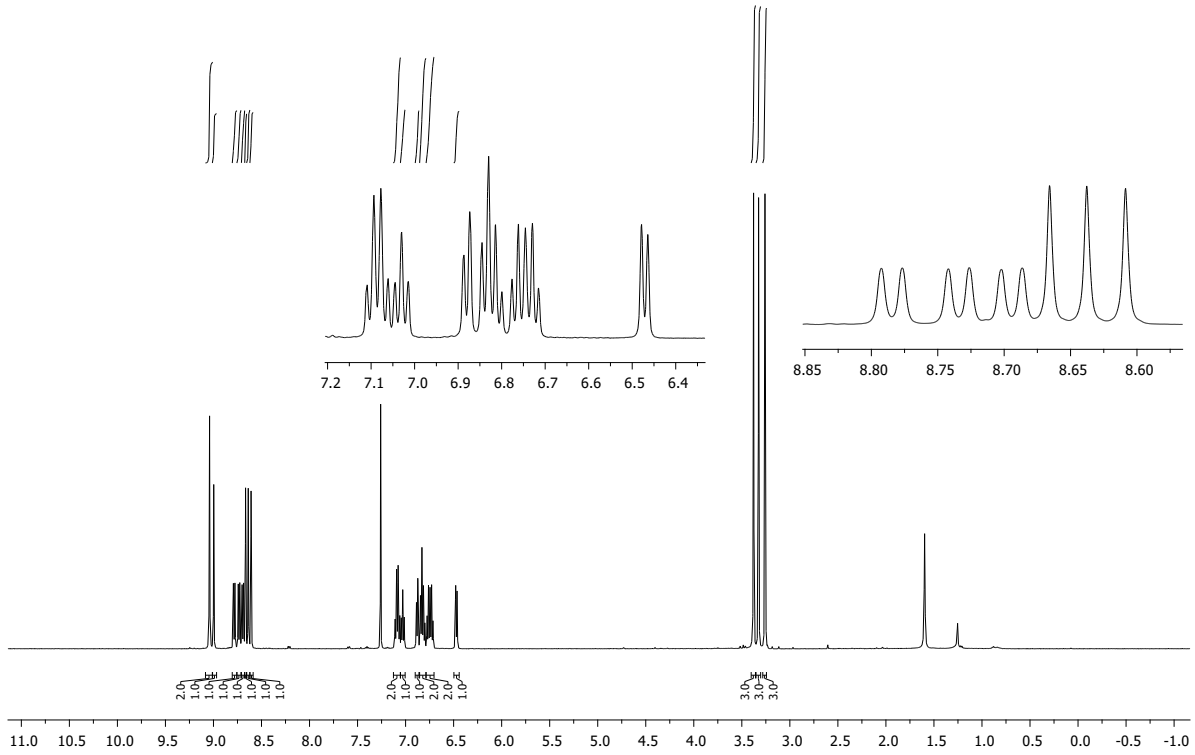

^{13}C-NMR (126 MHz, $CDCl_3$) spectrum of compound *mer*-PhP:

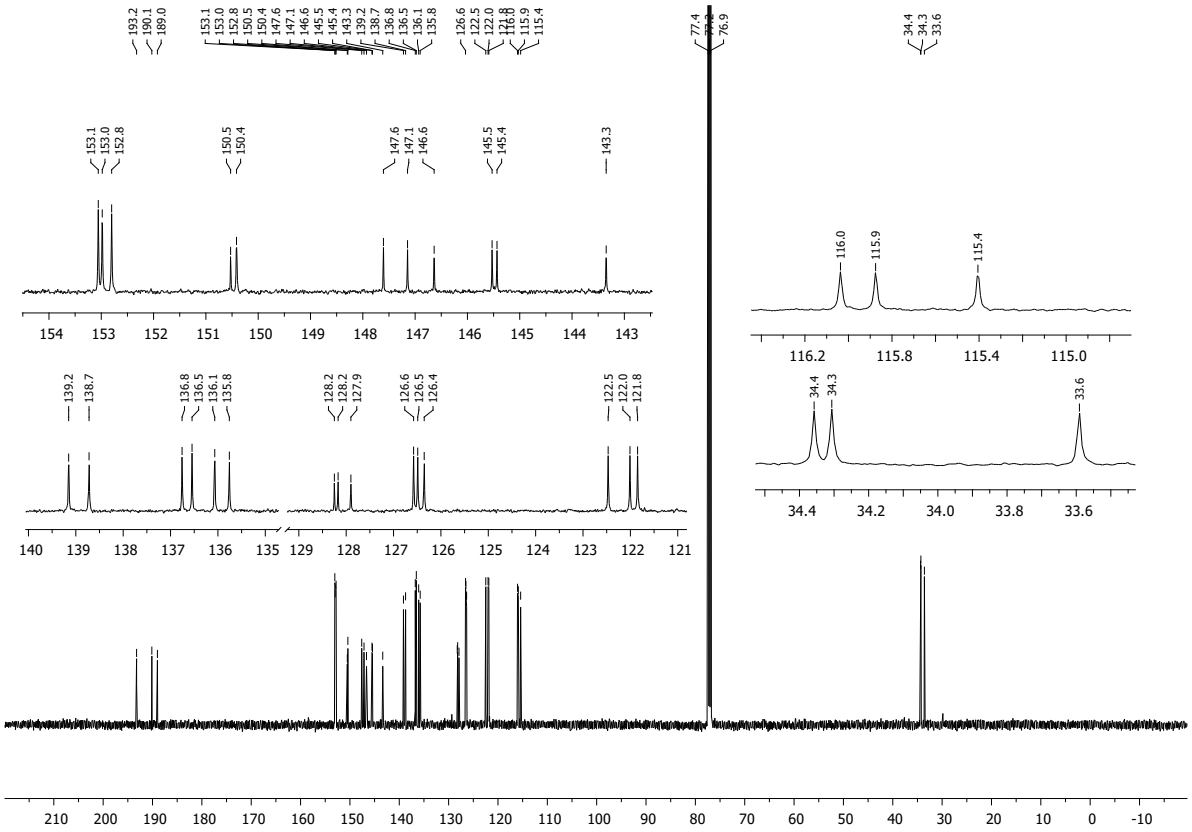

***Fac*-tris-(7-methyl-9-phenyl-purin-8-yl)iridium (*fac*-PhP)**

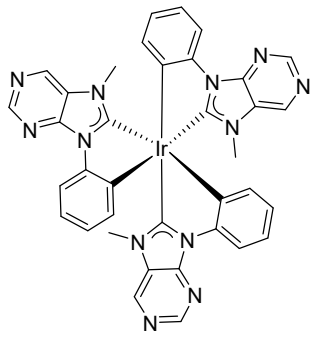

To a compound **7** (270 mg, 0.33 mmol, 1.0 eq.) solution in DCM (20 mL), EtOAc (40 mL) and 1M TFA (3.3 mL) were added and the mixture was stirred at 65 °C for 16 h in a pressure flask. Upon the completion reaction mixture was washed with sat. aq. $NaHCO_3$ (50 mL), H_2O (50 mL) and brine (25 mL). Organic layer was dried over anh. Na_2SO_4, filtered and evaporated. Silica gel column chromatography (DCM/EtOH gradient 0% → 10%) provided product ***fac*-PhP** (yield: 141 mg, 52%) as an off-white solid (90 mg, 33% of compound **7** was recovered). R_f = 0.20 (DCM/EtOH = 10:1). HPLC: t_R = 6.56 min. IR (KBr) ν (cm^{-1}): 3044, 1599, 1571, 1481, 1427, 1321, 1181. ^{1}H-NMR (500 MHz, $CDCl_3$) δ (ppm): 9.02 (s, 1H, H-C(2)), 8.75 (d, 1H, ^3J = 7.9 Hz, H-C(Ar)), 8.61 (s, 1H, H-C(6)), 7.14 (t, 1H, ^3J = 7.6 Hz, H-C(Ar)) 6.80 (t, 1H, ^3J = 7.4 Hz, H-C(Ar)), 6.51 (d, 1H, ^3J = 7.4 Hz, H-C(Ar)), 3.38 (s, 3H, (-CH_3)). ^{13}C-NMR (126 MHz, $CDCl_3$) δ (ppm): 194.7, 152.9, 150.6, 146.4, 144.6, 136.5, 136.2, 127.8, 126.5, 122.6, 115.5, 34.4. HRMS (ESI) m/z: $[M+H]^+$ Calcd for $C_{36}H_{28}N_{12}Ir$ 821.2189; Found 821.2180.

^{1}H-NMR (500 MHz, $CDCl_3$) spectrum of compound *fac*-PhP:

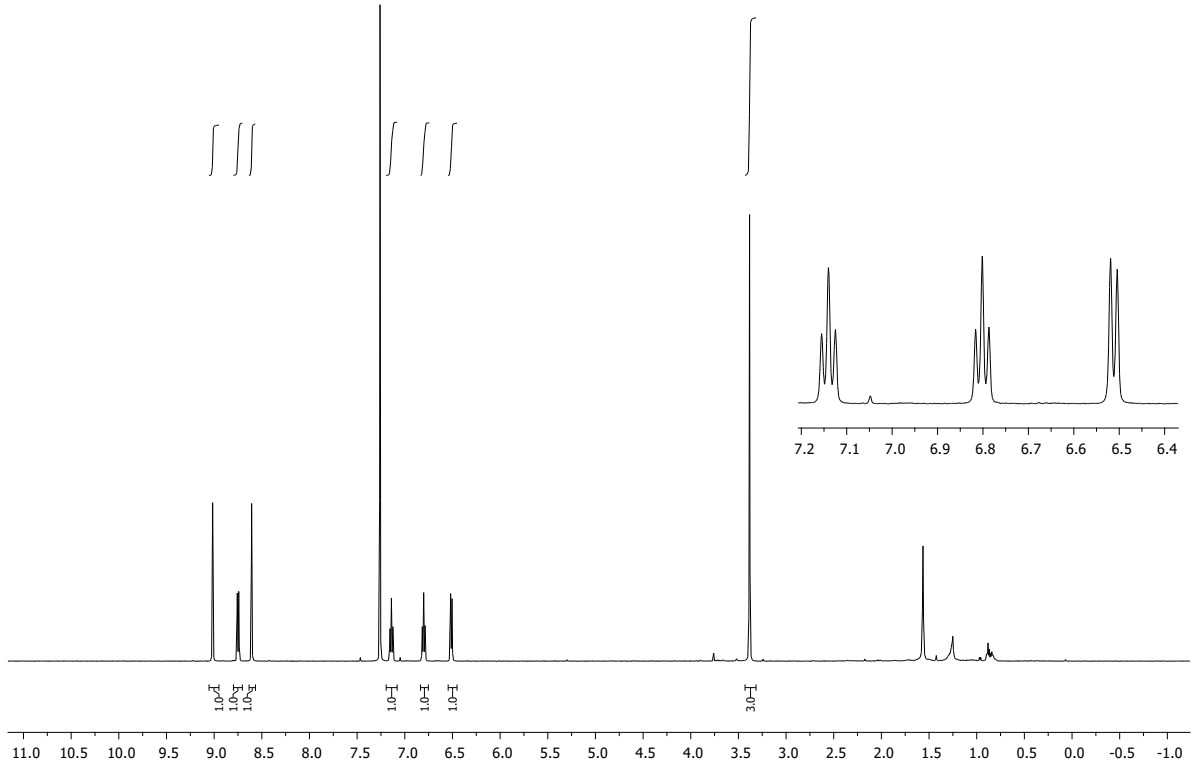

^{13}C-NMR (126 MHz, $CDCl_3$) spectrum of compound *fac*-PhP:

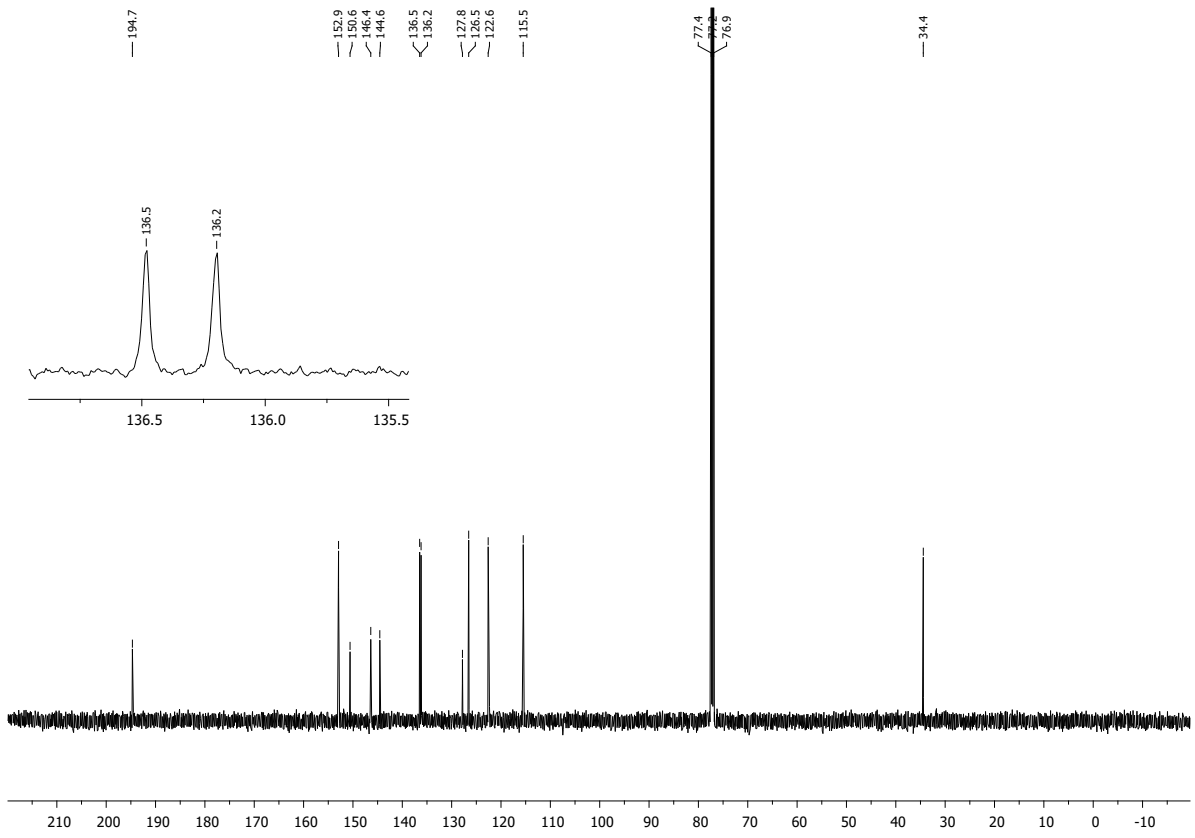

1.2. Thermal properties

Differential scanning calorimetry (DSC) measurements were recorded using TA Instruments DSC Q2000 equipment under a flow of nitrogen (40 mL/min) at heating and cooling rates of 10 °C/min. Thermogravimetric analyses (TGA) were performed on TA Instruments TGA Q50 apparatus by recording the weight loss within temperature range 20-800 °C at the rate of 20 °C/min under a nitrogen atmosphere (50 mL/min).

1.3. Photophysical characterizations

All solvents and materials were obtained from commercial sources and used as received, except when specified. UV−vis absorption and PL measurements were carried out in toluene (TOL) and dichloromethane (DCM) solutions with a material concentration of $1 \cdot 10^{-5}$ mol L^{-1}. Solutions for Φ_{PL} and emission decay measurements were prepared both in air saturated and deaerated solvents. Polymethylmethacrylate (PMMA) films for optical measurements were prepared from dichloromethane solution using a drop-casting method. The bulk samples of polystyrene (PS) were prepared by drying solutions in vacuum for a week at room temperature. The UV−vis spectra were recorded with a PerkinElmer Lambda 650 S spectrometer. PL spectra, Φ_{PL}, and PL lifetimes were obtained using QuantaMaster 40 spectrofluorometer (Photon Technology International, Inc.). Edinburgh Instruments FLS980 spectrometer equipped with PicoQuant LDH-DC- 375 laser (wavelength 374 nm) as the excitation source and Oxford Instrument Optistat DN2 cryostat and turbo-molecular pump (capable of achieving 10^{-5} Torr pressure) was used for temperature-dependent PL experiments.

The time-wavelength resolved luminescence set-up uses a frequency tripled Nd:YAG amplified laser system (30 ps, 30 mJ @1064 nm, 20 Hz, Ekspla model PL 2143; 10 mJ @355 nm). For longer timescales, a tunable nanosecond laser (5 ns, 135 mJ @355 nm from Nd:YAG amplified laser pumping OPO, 10 Hz, Ekspla model NT342B-10-WW) was used. The energy of light pulses @355nm were adapted for the best detection conditions. The luminescence signals were analyzed by a spectrograph (Princeton Instruments Acton model SP2300) coupled with a high dynamic range streak camera (Hamamatsu C7700, sweep ranges1ns-1ms, temporal resolution 30 ps @ 1 ns sweep range). Light signals were recorded and treated by HPDTA (Hamamatsu) software to produce two-dimensional maps (wavelength *vs* delay) of luminescence intensity in the range 300 – 800 nm. Later, data were analyzed using home-made

software developed in LabVIEW system-design platform and development environment. The fits in the case of temperature dependent measurements in PS samples were obtained using Levenberg–Marquardt algorithm of an analytical solution of a set of differential equations (1) describing the population changes in two successively populated electronic states following the Gaussian excitation pulse:

$$\begin{cases} \frac{dN_1}{dt} = G(t) - \frac{1}{\tau_1}N_1 \\ \frac{dN_2}{dt} = \frac{1}{\tau_1}N_1 - \frac{1}{\tau_2}N_2 \end{cases} \quad (1)$$

1.4. Fabrication and characterization of PhOLEDs

All of the functional materials (except iridium(III) complexes) which were used in the PhOLED structures were purchased from Sigma Aldrich or Lumtec companies and were used as received. Pre-patterned and pre-cleaned indium tin oxide (ITO) coated glass substrates with a sheet resistance of 15 Ω/sq were utilized for device fabrications. PhOLEDs with iridium(III) complexes as emitters were fabricated by vacuum deposition under the vacuum of ca. 10^{-6} mBar. All of the vacuum-evaporated layers were deposited at a rate of 1 Å s^{-1} except the LiF and MoO_3 layers which were deposited at 0.1 Å s^{-1} and also for all devices, layers were deposited at the same time except the light-emitting layers. Current density-Voltage-Luminance (JVL) characteristics were recorded using a calibrated photodiode PH100-Si-HA-D0 and sourcemeter Keithley 2400C together with the PC-Based power and energy monitor 11S-LINK. An Avantes (AvaSpec-2048XL) spectrometer was used to record electrophosphorescence spectra. The characteristics of brightness and current density as a function of voltage together with electrophosphorescence spectra were used to calculate fabricated device efficiencies.

1.5. Photoelectron emission spectroscopy

The solid-state ionization potential (IP^{PE}) was determined by using electron photoemission spectroscopy in the air and fluorine-doped tin oxide (FTO) coated glass slides were applied as substrates for the preparation of evaporated samples. Photoelectrical measurement setup

contained a deep UV deuterium light source (ASBN-D130-CM), CM110 1/8 m monochromator and Keithley 6517B electrometer/high resistance meter.

1.6. DFT calculations

Density functional theory (DFT) calculations for ground state geometry optimization and molecular orbital configurations, as well as time-dependent DFT (TD-DFT) calculations for the excited state energies T_1 geometries were performed using the Schrödinger Jaguar[1] software package (release 2022-1). Geometry optimization and TD-DFT calculations employed the PBE0[2] functional and the LACVP** basis. The Tamm–Dancoff approximation (TDA) was used for the TD-DFT. For TD-DFT calculations benzene served as a surrounding medium, introduced by conductor-like polarizable continuum model (CPCM). SOC-TD-DFT calculations were carried at the PBE0/ZORA-DEF2-TZVP theory level employing the Orca program package.[3]

Emissive rates for individual triplet state sublevels were obtained using the calculated oscillator strength *f* values following the equation:[4]

$$k_r = \frac{n^2 \tilde{\nu}_{em}^{\,2} f}{1.5} \tag{2}$$

where n is refractive index of surrounding medium and $\tilde{\nu}_{em}$ is the emission wavenumber.

Radiative lifetime as an average over the three triplet substates was calculated by:[5]

$$\tau_{total} = \frac{1}{k_{total}} = \left(\frac{1 + e^{-\left(\Delta E_{I,II}/k_B T\right)} + e^{-\left(\Delta E_{I,III}/k_B T\right)}}{k_I + k_{II} e^{-\left(\Delta E_{I,II}/k_B T\right)} + k_{III} e^{-\left(\Delta E_{I,III}/k_B T\right)}} \right) \tag{3}$$

where ΔE is energy gap between triplet substates, k_B is Boltzmann constant and T is temperature.

X-ray analysis

Table S1. Experimental details and crystal data for ***mer*-PhP**

Chemical formula	$C_{36}H_{27}IrN_{12}\cdot CH_2Cl_2$
M_r	904.82
Crystal system, space group	Monoclinic, $P2_1/c$
Temperature (K)	150
a, b, c (Å)	11.72923 (12), 14.3276 (3), 21.0437 (3)
β (°)	101.6081 (10)
V (Å^3)	3464.10 (8)
Z	4
Radiation type	Cu $K\alpha$
μ (mm^{-1})	9.27
Crystal size (mm)	0.10 × 0.08 × 0.06
Data collection	
Diffractometer	XtaLAB Synergy, Dualflex, HyPix
Absorption correction	Multi-scan *CrysAlis PRO* 1.171.40.71a (Rigaku Oxford Diffraction, 2020) Empirical absorption correction using spherical harmonics, implemented in SCALE3 ABSPACK scaling algorithm.
T_{min}, T_{max}	0.607, 1.000
No. of measured, independent and observed [$I > 2\sigma(I)$] reflections	32651, 6785, 6640
R_{int}	0.024
$(\sin\theta/\lambda)_{max}$ (Å^{-1})	0.631
Refinement	
$R[F^2 > 2\sigma(F^2)]$, $wR(F^2)$, S	0.021, 0.053, 1.09
No. of reflections	6785
No. of parameters	500
H-atom treatment	H-atom parameters constrained
$\Delta\rho_{max}$, $\Delta\rho_{min}$ (e Å^{-3})	0.62, -1.07
CCDC number	2269594

Table S2. Experimental details and crystal data for ***fac*-PhP**

Chemical formula	$C_{36}H_{27}IrN_{12}·CH_4O$[+solvent]
M_r	851.94
Crystal system, space group	Triclinic, $P\bar{1}$
Temperature (K)	150
a, b, c (Å)	8.8773 (1), 13.0655 (2), 16.2973 (2)
α, β, γ (°)	76.941 (1), 79.364 (1), 72.931 (1)
V (Å^3)	1746.02 (4)
Z	2
Radiation type	Cu $K\alpha$
μ (mm^{-1})	7.80
Crystal size (mm)	0.12 × 0.08 × 0.04
Data collection	
Diffractometer	XtaLAB Synergy, Dualflex, HyPix
Absorption correction	Multi-scan *CrysAlis PRO* 1.171.40.71a (Rigaku Oxford Diffraction, 2020) Empirical absorption correction using spherical harmonics, implemented in SCALE3 ABSPACK scaling algorithm.
T_{min}, T_{max}	0.406, 1.000
No. of measured, independent and observed [$I > 2\sigma(I)$] reflections	31696, 6946, 6880
R_{int}	0.058
$(\sin\theta/\lambda)_{max}$ (Å^{-1})	0.631
Refinement	
$R[F^2 > 2\sigma(F^2)]$, $wR(F^2)$, S	0.027, 0.071, 1.06
No. of reflections	6946
No. of parameters	467
H-atom treatment	H atoms treated by a mixture of independent and constrained refinement
$\Delta\rho_{max}$, $\Delta\rho_{min}$ (e Å^{-3})	0.81, -1.71
CCDC number	2269602

Thermal properties

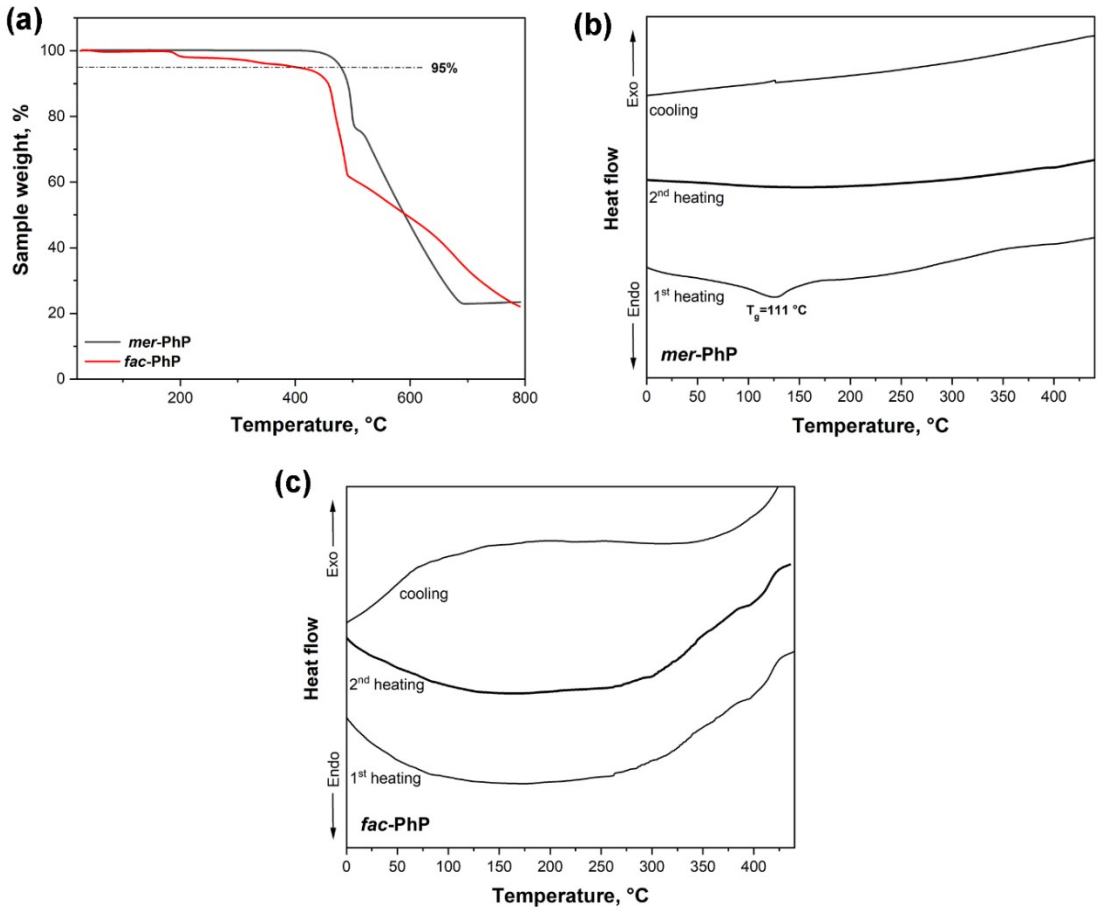

Figure S1. TGA and DSC curves of ***mer*-PhP** and ***fac*-PhP**.

Table S3. Thermal characteristics of ***mer*-PhP** and ***fac*-PhP.**

Compound	Samples	$T_{d\text{-}5\%}$, ºC [a]	T_g, ºC [b]	T_{cr}, ºC	T_m, ºC
***mer*-PhP**	Powder	480	111	-	-
***fac*-PhP**	Powder	402	-	-	-

[a] 5% weight loss temperature, determined by TGA (heating rate of 20 ºC min^{-1}; nitrogen atmosphere).

[b] estimated by first heating scan of DSC; (heating rate of 10 ºC min^{-1}; nitrogen atmosphere);

Table S4. Previously reported T_d values of NHC-based iridium(III) complexes.

Compound	T_d, °C	Reference
***mer*-Ir(tfpi_Bn)$_3$, *fac*-Ir(tfpi_Bn)$_3$**	380	6
5	425.8	7
B2	459	8
Ir2	469	9
2	396	10
***mer*-Ir1**	392	11

Temperature dependent PL measurements in doped polymer films

Regarding PL intensity, in the case of ***mer*-PhP** no notable temperature-induced changes can be observed for the film of its solid solutions in PMMA. In contrast, for ***fac*-PhP** upon cooling quantum yield increases from 0.77 to near unity, indicating that at room temperature conditions a partial thermal population of nonradiative states takes place.[12] In order to gain a better understanding about light emission quenching effects induced by thermal energy, time-dependent PL measurements in PS guest host systems were carried at 4 °C, 36 °C and 66°C. The samples were excited at 355 nm with 5 ns laser pulses and the emission was recorded with the streak camera at 100 nm sweep range and 2–10 μs sweep range. The acquired time-wavelength resolved emission intensity maps for 100 ns sweep range are presented in Fig. S2. Two principal features are present in all maps: i) a blue shifted emission band growing with the excitation pulse and relaxing within 20 ns range and ii) a redshifted longer living (exceeding 200 ns) emission band (Fig. S3, Table S5). These emissive processes can be attributed to two local minima on T_1 state potential energy surface. Upon temperature increase both complexes show a decrease in PL intensity, although this effect is much more pronounced for ***mer*-PhP**. Regarding the observed spectral profile, for ***fac*-PhP** both emissive processes have almost identical wavelength and FWHM values and no notable variations with temperature changes take place. For ***mer*-PhP**, however, longer lived PL component is significantly redshifted and broadened and upon heating experiences a disproportionally larger drop in intensity. This may indicate a further excitation transfer from redshifted PL component to the non-emissive global minima of T_1 state upon thermal activation. In addition, the plasticization of PS matrix and loss of molecular rigidity may also contribute to the more pronounced decrease in PL efficiency for ***mer*-PhP**.

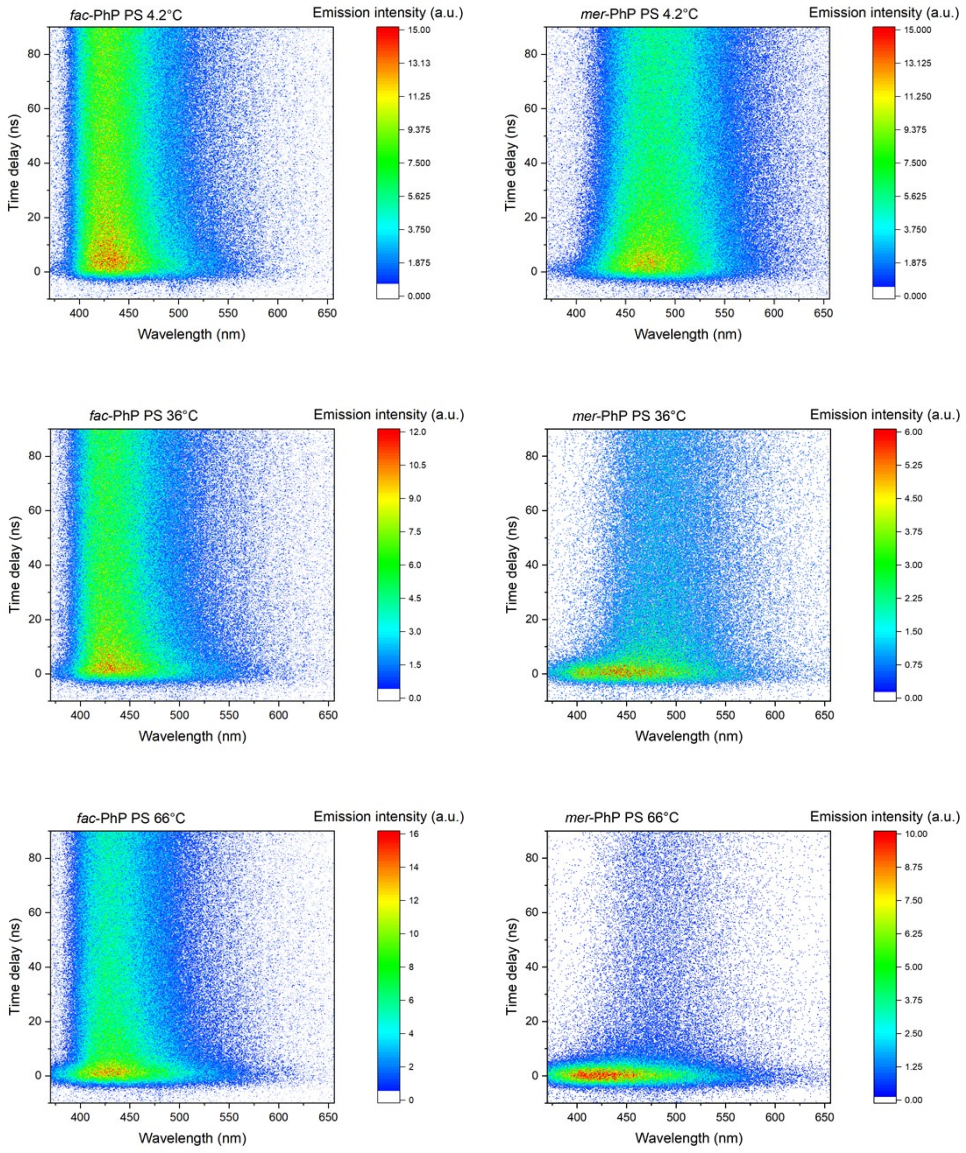

Figure S2. Time wavelength resolved emission intensity maps of PS samples containing 5 wt% of emitter at different temperatures.

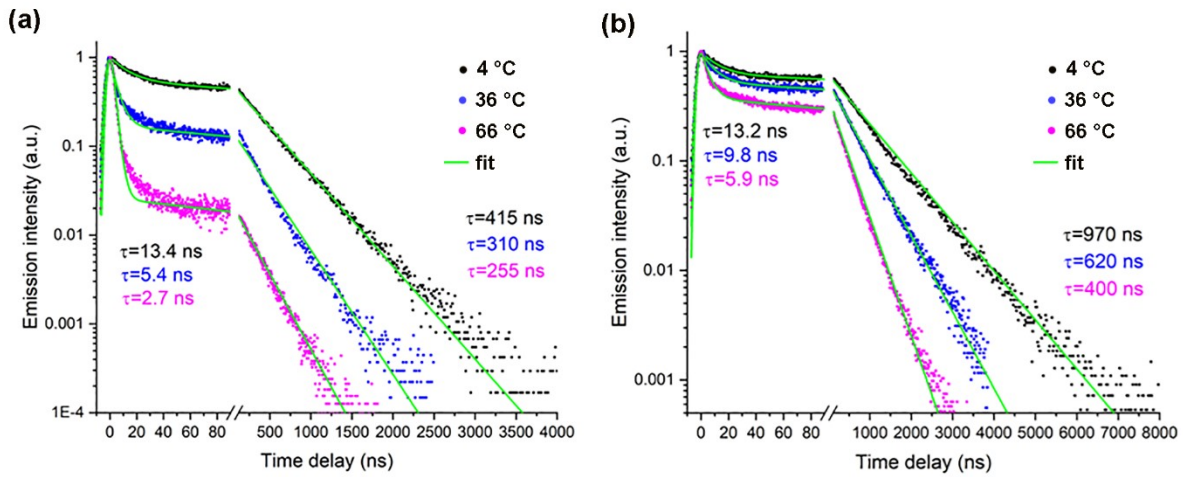

Figure S3. Emission kinetic and fits for ***mer*-PhP** (a) and ***fac*-PhP** (b) at various temperatures.

Photophysical properties

Table S5 Photophysical properties of PS samples containing 5 wt% of emitter at different temperatures.

Compound	***fac*-PhP**			***mer*-PhP**		
T, °C	4	36	66	4	36	66
λ_{max} at 0 ns, nm	430	430	428	472	447	421
FWHM at 0 ns, nm	67	75	82	84	88	91
λ_{max} >200 ns, nm	430	430	430	483	484	484
FWHM > 200 ns, nm	65	60	61	84	77	77
τ_1, ns	13.2	9.8	5.9	13.4	5.4	2.7
τ_2, ns	970	620	400	415	310	255

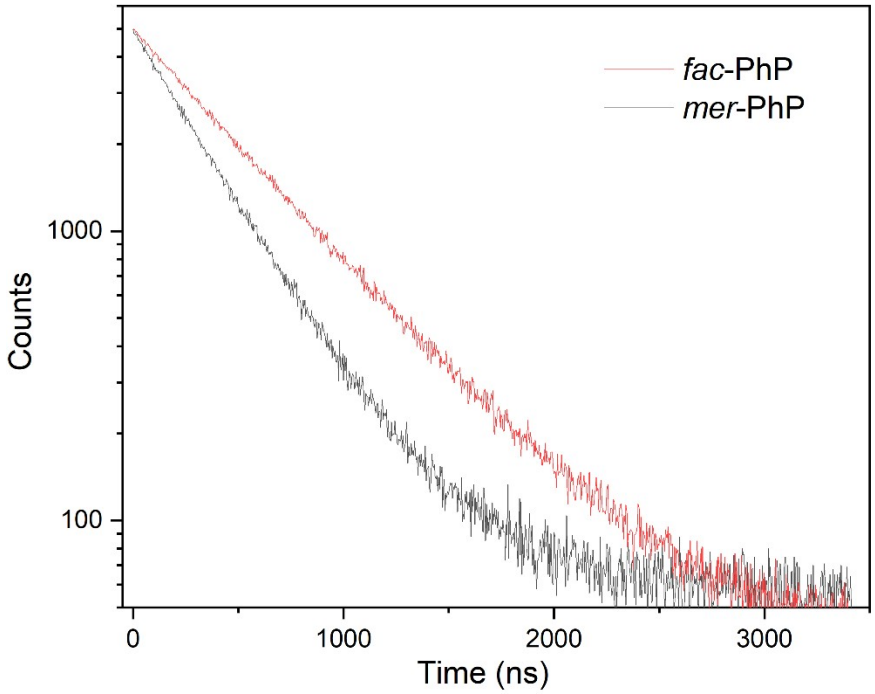

Figure S4. PL decay of ***mer*-PhP** and ***fac*-PhP** measured in DCM.

Table S6 Temperature dependent PL measurements of ***mer*-PhP** and ***fac*-PhP** in doped PMMA films (5 wt%).

	Temperature, K					
	300	250	200	150	100	77
			***mer*-PhP**			
Φ_{PL}	0.99	0.99	0.99	0.99	0.99	0.99
τ, ns	880	985	1053	1184	1408	1531
k_r, $1 \cdot 10^5$ s^{-1}	11.3	10.1	9.4	8.4	7.0	6.5
			***fac*-PhP**			
Φ_{PL}	0.77	0.99	0.99	0.97	0.95	0.95
τ, ns	940 (60%), 2226 (40%)	1053 (53%), 2686 (47%)	1468 (47%), 4528 (53%)	1702 (40%), 5721 (60%)	2407 (35%), 8125 (65%)	2804 (36%), 8927 (64%)
k_r, $1 \cdot 10^5$ s^{-1}	4.9, 1.4	5.0, 1.8	3.2, 1.2	2.3, 1.0	1.4, 0.7	1.2, 0.6

DFT Calculations

Table S7 Metal-ligand bond length values for DFT optimized (PBE0, LACVP**) and experimental X-ray structures.

Bond	***mer*-PhP** (X-ray)	***fac*-PhP** (X-ray)	***mer*-PhP** (calc. S_0)	***fac*-PhP** (calc. S_0)	***mer*-PhP** (calc. T_1)	***fac*-PhP** (calc. T_1)
Ir-C1	2.036	2.028	2.04	2.01	2.15*	2.06*
Ir-C2	2.112	2.092	2.11	2.10	2.10*	2.06*
Ir-C3	2.017	2.013	2.00	2.01	2.03	2.09
Ir-C4	2.081	2.081	2.08	2.10	2.04	2.09
Ir-C5	2.018	2.022	2.03	2.01	2.02	2.06
Ir-C6	2.106	2.093	2.10	2.10	2.05	2.04

* Indicated are bonds with the ligand, which hosts electron after MLCT transition process.

The alignment of the frontier molecular orbitals is governed by the symmetry group of the complex molecules. For C_1 symmetric ***mer*-PhP** the highest occupied molecular orbital (HOMO) is predominantly located on Ir atom and one of the phenyl rings of a phenylpurine ligand, while the lowest unoccupied molecular orbital (LUMO) is placed on a purine ring, which is positioned opposite to the HOMO-hosting phenyl (Fig. 6a). For C_3 symmetric ***fac*-PhP** the orbital configuration is similar, but both HOMO and LUMO are evenly distributed across all three phenyl or purine rings. Considering the energy level values, in ***mer*-PhP** HOMO is destabilized by 0.20 eV, while LUMO is stabilized by 0.15 eV, decreasing the HOMO-LUMO gap by 0.35 eV in comparison to ***fac*-PhP**.

Sequentially, TD-DFT calculations were performed to characterize the electronic excitation processes. $S_0 \rightarrow S_1$ transition energies were calculated at ground state geometry (Fig. 6b). Natural transition orbitals (NTOs) relate the lowest energy singlet state to MLCT process, where electron transfer proceeds from predominantly metal-dominated HONTO orbital to ligand-centered LUNTO. In agreement with the experimental observations a slight redshift (by 0.06 eV) in ^{1}MLCT absorption band is predicted in the case of ***mer*-PhP**.

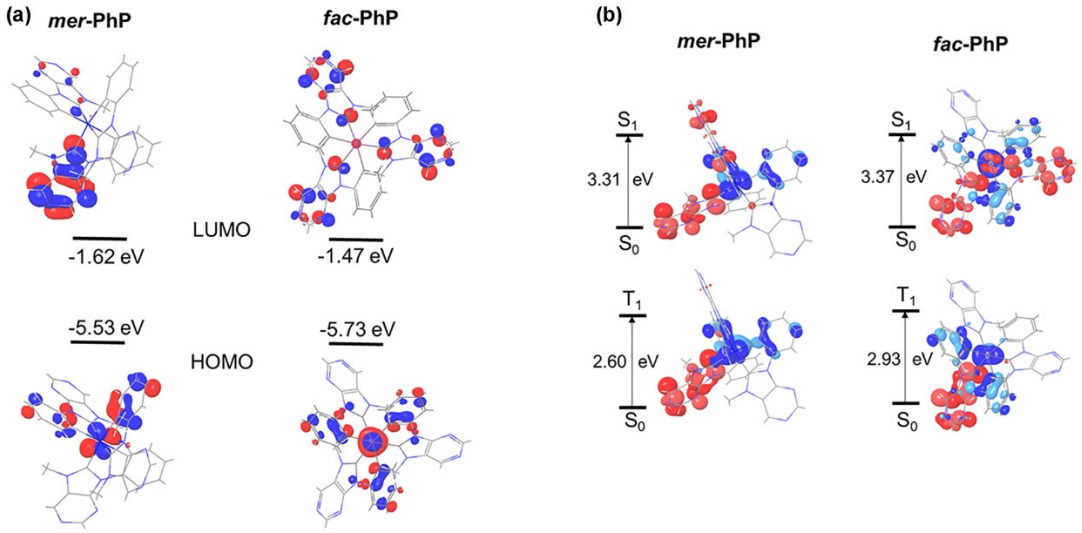

Figure S5. (a) HOMO and LUMO orbitals and their energy level values. (b) Natural transition orbitals (NTOs) of S_1 and T_1 excitations. Blue regions visualize hole, while red correspond to particle.

Table S8 Calculated molecular orbital contributions to lowest energy singlet and triplet excitations (PBE0/ZORA-DEF2-TZVP).

Compound	Excitation	Molecular orbital assignment ([%])[a]	Ir atom contribution (%)[b]
***mer*-PhP**	$S_0 \rightarrow S_1$	HOMO→LUMO (97)	35
	$S_0 \rightarrow T_1$	HOMO→LUMO (95)	
***fac*-PhP**	$S_0 \rightarrow S_1$	HOMO→LUMO (89)	33
	$S_0 \rightarrow T_1$	HOMO→LUMO (89)	

[a] Contribution in percents of corresponding molecular orbital transitions towards total excitation. Contributions over 5% are given. Contributions over 5% are given. [b] Contribution of the metal atom to corresponding molecular orbital transitions, calculated with Becke method (Multiwfn).

Electrical and electroluminescent properties

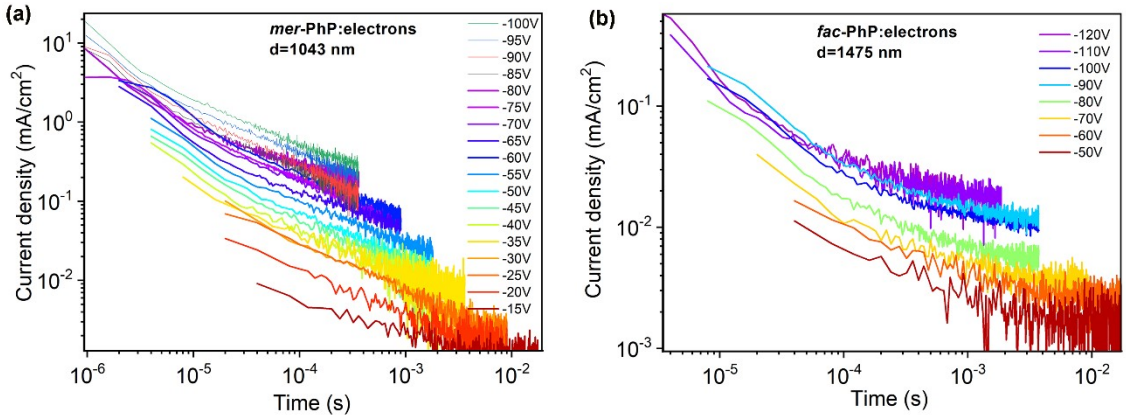

Figure S6. TOF transients for electrons for the layers of ***mer*-PhP** (a) and ***fac*-PhP** (b) recorded at the different voltages applied to ITO. t_{tr} were not observed.

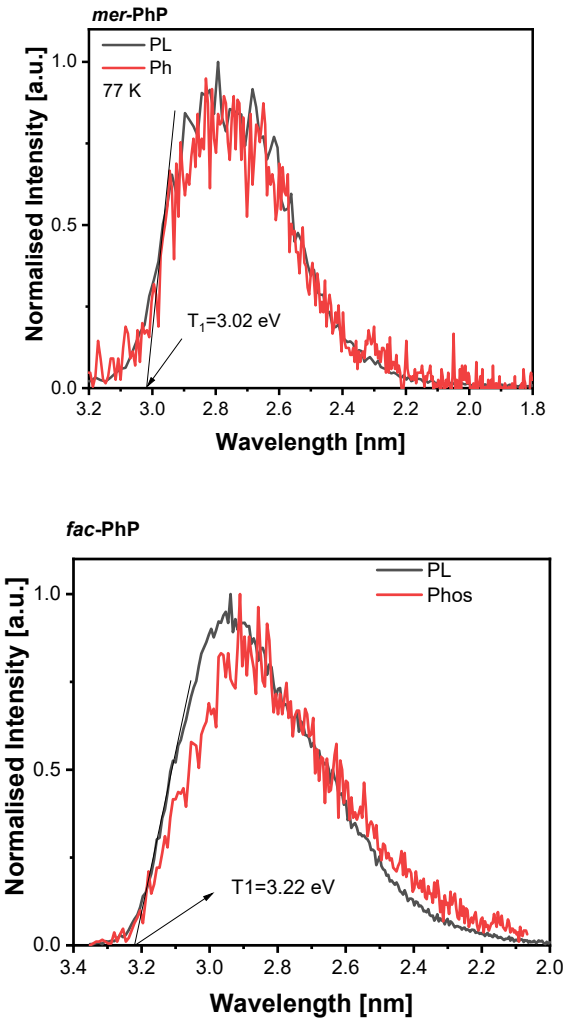

Figure S7. PL spectra of the Me-THF solution of the complexes at 77K. The phosphorescence (Phos.) spectra was recorded with delay of 1 ms after excitation.

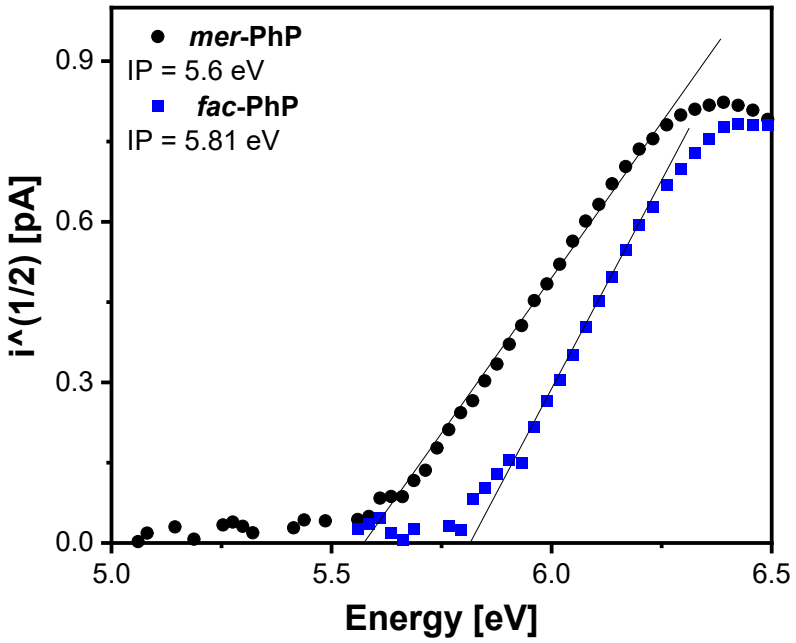

Figure S8. Photoelectron emission spectra of the neat film of the complex ***mer*-PhP** and ***fac*-PhP**.

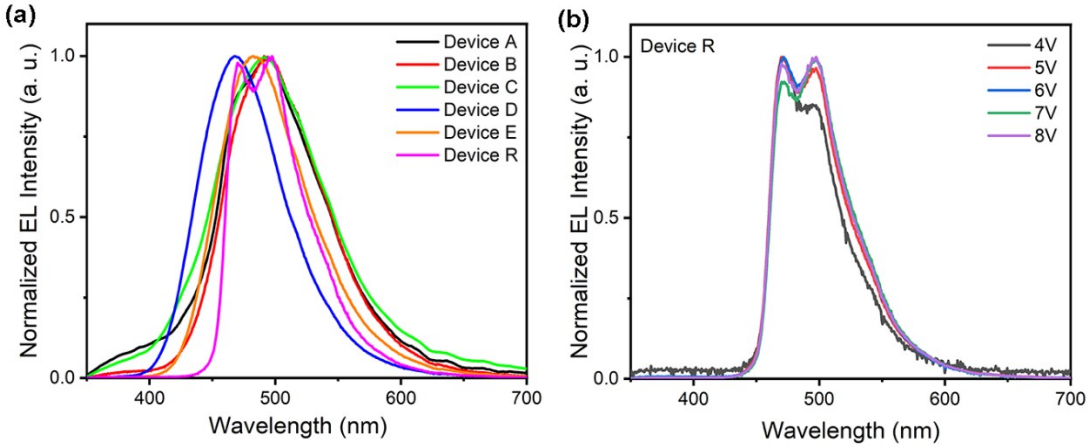

Figure S9. EL spectra of the devices A-E and R at 8 V (a). EL spectra of device R recorded at different driving voltages (b).

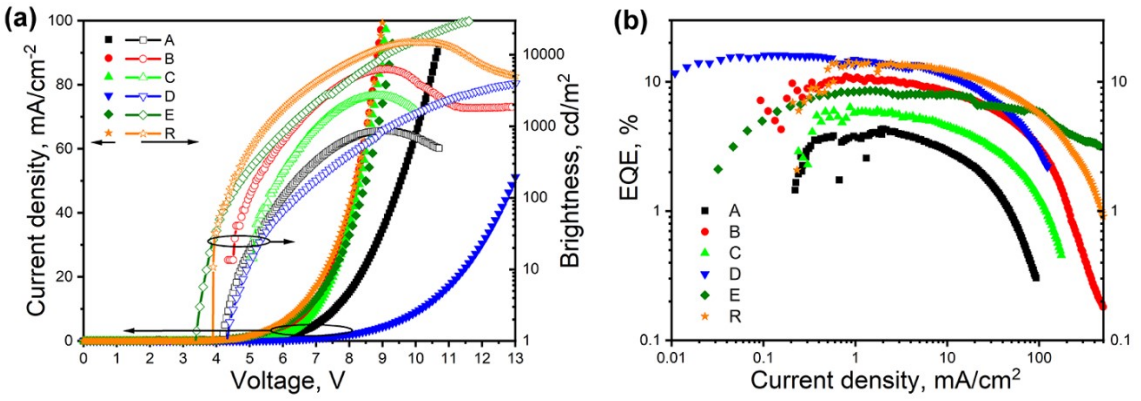

Figure S10. Plots of current density and brightness versus external voltage (a), plot of EQE versus current density (b) for devices A-E and R.

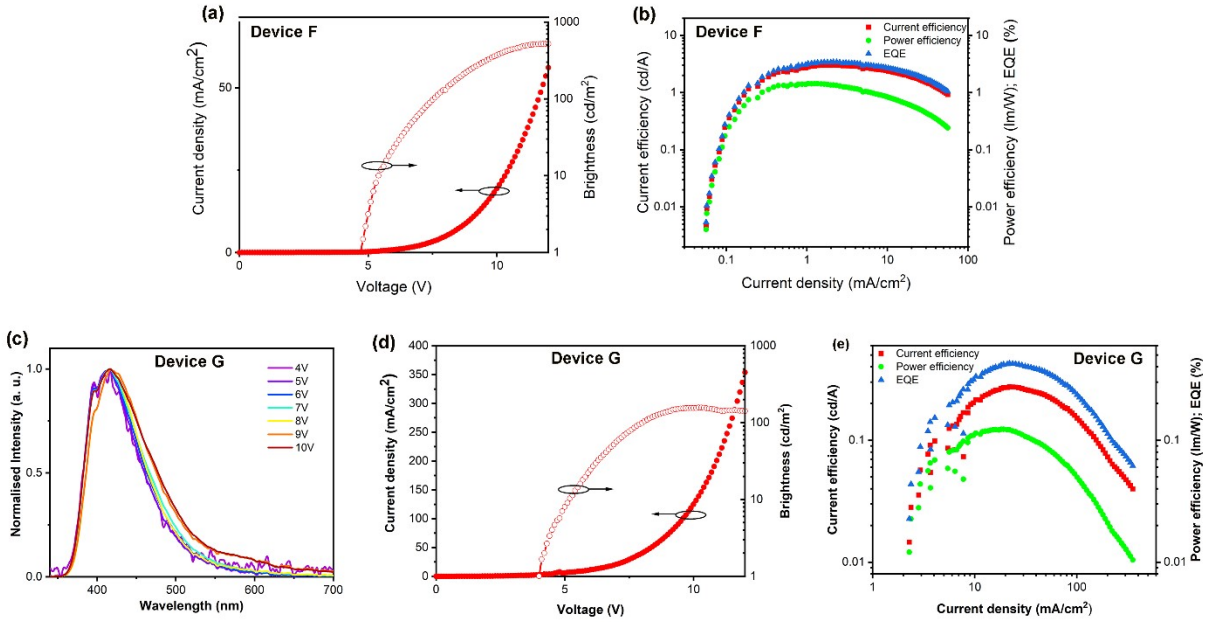

Figure S11. EL spectra at different voltages, dependencies of current density and brightness versus external voltage, current efficiency, power efficiency and EQE plots as the function of current density for ***fac*-PhP** based device F and G.

Table S9. Output electrophosphorescence parameters of the similar previously published devices.

Device	**EML**	λ, nm	V_{ON},[a] V	L_{MAX},[b] cd/m^2	CE_{MAX},[c] cd/A	PE_{MAX},[d] lm/W	EQE_{MAX},[e] %	Ref.
Structure: ITO/TAPC/TCTA/mCP/**EML**/3TPYMB/LiQ/Al								13
L1	*f*-2tBu (14wt%):PPF	440	3.6	-	7.7	-	7.5	
L2	*m*-2tBu (14wt%):PPF	482	3.5	-	35.2	-	17	
Structure: ITP/TAPC/**EML**/TmPyPB/LiF/Al								14
L3	*f*-CF_3 (15wt%):mCBP	478	4.7	5718	19.2	12.6	10.4	
L4	*f*-PhCF_3 (15wt%):mCBP	495	5.0	10769	32.6	19.7	12.8	

[a] Voltage, at which luminance 1 cd/m^2 was reached. [b] Maximal attained luminance. [c] Maximal current efficiency. [d] Maximal power efficiency. [e] Maximal external quantum efficiency.

DFT optimized molecular geometries

***mer*-PhP** S_0 geometry:

atom	x	y	z
Ir1	-0.1299256690	-0.2222288124	0.1291821912
N2	-2.3490073845	1.7934002532	1.0463108730
C3	3.1786531651	-2.5397573802	-1.2335015284
N4	0.5515847756	1.9627258336	-1.6805450853
N5	-2.8479034984	-0.3355935590	1.1208893037
C6	0.3743226042	-0.1446454319	3.2692821641
H7	-0.5590541087	0.4044122159	3.3814730065
N8	2.3406437309	-1.6697405072	0.6300972544
C9	-3.4979940885	-2.7097659813	1.1937288314
H10	-4.4824810163	-2.4558984216	1.5714974412
C11	-0.8336761491	1.6953019555	-3.7022510477
H12	-0.3929695766	2.5765474469	-4.1558844697
N13	-5.1777362902	-0.1409666403	1.8143960425
N14	1.7973669517	2.3174100807	0.0847354139
C15	-0.4320197373	1.2698669842	-2.4392059301
C16	-3.1267150036	-4.0299303572	0.9559196927
H17	-3.8314919793	-4.8321959146	1.1537904509
N18	4.4267450841	-2.9277566622	0.7918000440
C19	-3.6740838718	1.7058375718	1.4270971756
C20	-2.5668093634	-1.7118168106	0.9272865732
C21	2.3378920468	-1.1173264318	4.3004539790
H22	2.9323114320	-1.3293268309	5.1843098343
C23	0.8367364913	1.4896220064	-0.4145552396
C24	0.7781422845	-0.5457161899	1.9893918165
C25	-3.9909470757	0.3371193396	1.4805975317
C26	-1.9365185076	-0.5652632416	-2.4764811842
H27	-2.3722122673	-1.4482365290	-2.0137679957
N28	5.1694310229	-3.7809933214	-1.3284832461
C29	3.3918926640	-2.4125721435	0.1478651171
N30	1.3530036995	3.8081098610	-3.0639503227
N31	2.0063312843	-1.8717477948	-1.5240416564
C32	2.9974431955	4.3594917354	-0.8828444341
H33	3.6615481480	4.6141085258	-0.0592182515
C34	-0.9391808635	0.1330821445	-1.7856493825
C35	-6.0689880825	0.8153366703	2.0959919337
H36	-7.0622660804	0.4706723652	2.3737701123
C37	1.4466524233	-1.7879718737	-2.8564945454
H38	1.4635909596	-2.7796889716	-3.3167210571
H39	2.0250878960	-1.0921172428	-3.4712465695
H40	0.4191777550	-1.4369232131	-2.7822399714
C41	1.4882879559	-1.3232307232	-0.3943076402
C42	2.1222485531	3.2899211657	-0.8389237702
C43	4.1164065055	-3.2510110271	-1.9593564826
H44	4.0417180810	-3.4019876603	-3.0344683146
C45	5.2646846602	-3.5934850146	-0.0100924773
H46	6.1324714023	-4.0354161832	0.4739688745
C47	2.4104157180	2.2236168139	1.3925149298
H48	1.8457681441	1.5109083551	1.9918364199
H49	2.3969075947	3.2066929009	1.8727509666

H50	3.4455646825	1.8798108065	1.3064302741
N51	-5.8908331012	2.1376990431	2.0756607911
C52	-4.6821159536	2.5996546646	1.7367775879
H53	-4.5464354507	3.6793479282	1.7134412861
C54	-1.2695276633	-1.9381644743	0.4355519200
C55	-1.8524220582	-4.3107930163	0.4695881998
H56	-1.5592159588	-5.3420186479	0.2861986622
C57	-1.8126075973	0.9534744109	-4.3578454413
H58	-2.1445901429	1.2593208293	-5.3460529030
C59	-0.9452652033	-3.2813043888	0.2174025806
H60	0.0427413271	-3.5399211786	-0.1582400262
C61	1.3216665985	3.0640225982	-1.9699093463
C62	1.9852395168	-1.2662491091	1.9449642893
C63	-2.3654664041	-0.1677906122	-3.7435079114
H64	-3.1361789742	-0.7389582804	-4.2561253411
C65	1.1366607938	-0.4197413533	4.4057842814
H66	0.7887512327	-0.0875160420	5.3813616762
N67	3.0449217982	5.1247662761	-1.9789407092
C68	-1.6389441922	3.0267100278	0.7980585923
H69	-1.5965950503	3.2385138093	-0.2744967620
H70	-0.6260399152	2.9413586346	1.1918288995
H71	-2.1511776385	3.8436902162	1.3090185188
C72	2.7744826271	-1.5570212115	3.0530580994
H73	3.6988130791	-2.1134854440	2.9406217682
C74	2.2346452795	4.8116850133	-2.9919895538
H75	2.2967907551	5.4508078178	-3.8697049800
C76	-1.8389190795	0.5506372265	0.8368661199

***mer*-PhP** T_1 geometry:

atom	x	y	z
Ir1	-0.0157567612	-0.3093994488	0.1294873030
N2	-2.1795040777	1.8348182424	1.0341444499
C3	3.2257570018	-2.8105625224	-1.0816963954
N4	0.3786222891	2.0478962826	-1.6355562196
N5	-2.7755796869	-0.2658908694	0.9935312114
C6	0.5586761482	0.1599320737	3.1692454919
H7	-0.2753014609	0.8577251518	3.1919611006
N8	2.3659787713	-1.8408710938	0.7176741255
C9	-3.5252748091	-2.6017750953	0.9612240680
H10	-4.5078402038	-2.3212639362	1.3245825156
C11	-1.0867474534	1.7527386823	-3.5824417795
H12	-0.7902265630	2.7211301617	-3.9712922714
N13	-5.1267699585	-0.0015547945	1.5943606607
N14	1.8101966549	2.3792242425	-0.0141761108
C15	-0.5565311105	1.2998978847	-2.3773034787
C16	-3.1987937959	-3.9273060792	0.6808468824
H17	-3.9458062452	-4.7016800731	0.8298834324
N18	4.3434595221	-3.2373426993	1.0213340901
C19	-3.5260989410	1.7893156028	1.3521509759
C20	-2.5529449403	-1.6352241980	0.7503492280
C21	2.3063949787	-1.0362437373	4.3275313282
H22	2.8309546615	-1.2715467279	5.2493069034
C23	0.9135257418	1.4572282695	-0.5077301021

C24	0.9290651193	-0.4186617706	1.9419727798
C25	-3.9077508141	0.4402649726	1.3338353198
C26	-1.7994275638	-0.7269037927	-2.5007148436
H27	-2.0899462717	-1.6947088660	-2.1020670491
N28	5.1360715248	-4.1840108869	-1.0450499604
C29	3.3845252742	-2.6713503597	0.3042277977
N30	0.6492608724	4.1676154017	-2.8187417253
N31	2.1211998865	-2.0605211132	-1.4435560580
C32	2.5428831207	4.7008237729	-0.8076344130
H33	3.2971508191	4.9503163890	-0.0669232475
C34	-0.8795592901	0.0617304093	-1.8007196663
C35	-5.9863331971	0.9873642530	1.8774675385
H36	-7.0058501203	0.6791606716	2.0964359388
C37	1.6607929640	-1.9177699542	-2.8074740667
H38	1.4561569863	-2.9040587616	-3.2351554556
H39	2.4239919114	-1.4160778595	-3.4102850965
H40	0.7472511934	-1.3240868677	-2.8060873838
C41	1.5790659431	-1.4594005850	-0.3525591980
C42	1.8268724656	3.5090671892	-0.8054564562
C43	4.1503284930	-3.5983714075	-1.7527330196
H44	4.1250273533	-3.7663490457	-2.8261413519
C45	5.1777577436	-3.9781821344	0.2645983785
H46	5.9876055425	-4.4659439503	0.8025843476
C47	2.7474586452	2.1848427866	1.0639639290
H48	2.4648673322	1.3017855839	1.6328075919
H49	2.7356732431	3.0558692748	1.7270466332
H50	3.7624556824	2.0560911684	0.6713063893
N51	-5.7473265940	2.2974339698	1.9200804087
C52	-4.5048377686	2.7211016939	1.6531433195
H53	-4.3198834301	3.7926760589	1.6765973346
C54	-1.2463823458	-1.9231385201	0.2875481418
C55	-1.9293308005	-4.2617453781	0.2060404605
H56	-1.6890707483	-5.2993721364	-0.0092909248
C57	-1.9915449082	0.9333466371	-4.2506233053
H58	-2.4179167929	1.2644701058	-5.1934429744
C59	-0.9751830921	-3.2718717893	0.0016003794
H60	0.0023787108	-3.5472493058	-0.3843043417
C61	0.9054862785	3.3015542935	-1.8428920737
C62	2.0398840399	-1.3037177969	1.9727203896
C63	-2.3446307931	-0.3005358840	-3.7136422764
H64	-3.0507892630	-0.9399489152	-4.2380597870
C65	1.2269218736	-0.1480074228	4.3469878486
H66	0.9118134610	0.2988836609	5.2861635369
N67	2.2958337314	5.5999110856	-1.7925568511
C68	-1.4182447991	3.0609749318	0.9194313429
H69	-1.5147453871	3.4874463218	-0.0833600325
H70	-0.3697073541	2.8422436179	1.1156069134
H71	-1.7850256345	3.7763096403	1.6587821671
C72	2.7243161477	-1.6279573986	3.1369085115
H73	3.5574486215	-2.3219966460	3.1043491920
C74	1.3929434776	5.2934799469	-2.7069573283
H75	1.2215261974	6.0385177347	-3.4818125267
C76	-1.7156914958	0.5866197946	0.7909731684

***fac*-PhP** S_0 geometry:

atom	x	y	z
Ir1	-0.0000000000	-0.0000000000	0.2799607449
C2	-1.3903802848	-4.0671429915	2.6794443953
C3	-2.1119402646	-3.5399280559	1.6120282186
C4	-1.6351111306	-2.3752241452	1.0180041242
C5	-0.4720144941	-1.6956931911	1.4199449275
C6	0.2193150007	-2.2642468124	2.4931815702
C7	-0.2315098017	-3.4287885331	3.1165077737
H8	-1.7370772148	-4.9738629881	3.1667145757
H9	-3.0215303175	-4.0095039759	1.2533987028
H11	1.1240871360	-1.7791280460	2.8512962902
H12	0.3285095875	-3.8413163416	3.9525481049
C13	-2.8270590091	3.2376761434	2.6794443953
C14	-2.8536630730	1.9148876360	3.1165077737
C15	-2.0705527603	0.9421910442	2.4931815702
C16	-1.2325061335	1.2566231384	1.4199449275
C17	-1.2394488841	2.6036598498	1.0180041242
C18	-2.0096974917	3.5989579484	1.6120282186
H19	-3.4389530952	3.9912844904	3.1667145757
H20	-3.4909323296	1.6361605226	3.9525481049
H21	-2.1028136525	-0.0839239929	2.8512962902
H23	-1.9615671410	4.6214740012	1.2533987028
C24	4.2174392939	0.8294668482	2.6794443953
C25	3.0851728747	1.5139008970	3.1165077737
C26	1.8512377596	1.3220557682	2.4931815702
C27	1.7045206276	0.4390700527	1.4199449275
C28	2.8745600148	-0.2284357045	1.0180041242
C29	4.1216377563	-0.0590298925	1.6120282186
H30	5.1760303100	0.9825784977	3.1667145757
H31	3.1624227420	2.2051558190	3.9525481049
H32	0.9787265164	1.8630520389	2.8512962902
H34	4.9830974585	-0.6119700253	1.2533987028
C35	-1.7020979066	-0.6234243486	-0.5963863136
N33	-2.2988572136	-1.7440015018	-0.0682182827
N34	-2.5456569358	-0.1627969069	-1.5619080602
C45	1.3909502765	-1.1623478526	-0.5963863136
N36	1.4138147249	-2.1232051223	-1.5619080602
N37	2.6597782116	-1.1188679958	-0.0682182827
C55	0.3111476301	1.7857722012	-0.5963863136
N39	1.1318422109	2.2860020292	-1.5619080602
N40	-0.3609209980	2.8628694976	-0.0682182827
C41	0.2576017126	-2.5591638237	-2.3101128493
C42	-2.3451017401	1.0564922847	-2.3101128493
C43	2.0875000275	1.5026715390	-2.3101128493
C56	2.6697126631	-2.6933894730	-1.6401005452
C57	3.4704495998	-2.0400011953	-0.6866319275
N46	4.7508180632	-2.3018536568	-0.4842770375
C59	5.2222134943	-3.2690753874	-1.2793229595
N48	4.5637142115	-3.9625881362	-2.2093515248
C61	3.2693118100	-3.6813844090	-2.3983248826
H65	6.2725248297	-3.5191342753	-1.1495840030
H67	2.7354501609	-4.2564699402	-3.1524969531

C62	-3.5019176588	-1.9854969183	-0.6866319275
C63	-3.6674000374	-0.9653442506	-1.6401005452
C64	-4.8228283243	-0.9906148758	-2.3983248826
N57	-5.7135590964	-1.9709983747	-2.2093515248
C66	-5.4422090795	-2.8880318563	-1.2793229595
N59	-4.3688727741	-2.9634023031	-0.4842770375
H70	-5.0539361791	-0.2407343600	-3.1524969531
H72	-6.1839220966	-3.6725987107	-1.1495840030
C68	0.9976873743	3.6587337236	-1.6401005452
C69	0.0314680590	4.0254981137	-0.6866319275
N66	-0.3819452890	5.2652559598	-0.4842770375
C71	0.2199955852	6.1571072438	-1.2793229595
N68	1.1498448849	5.9335865109	-2.2093515248
C73	1.5535165143	4.6719992849	-2.3983248826
H77	-0.0886027331	7.1917329860	-1.1495840030
H79	2.3184860182	4.4972043002	-3.1524969531
H68	2.2967872996	1.9975764992	-3.2610255062
H69	3.0169029662	1.3831728367	-1.7451700496
H71	1.6596939114	0.5185098409	-2.5029097848
H73	-2.8783456441	0.9902878989	-3.2610255062
H74	-2.7063142975	1.9211281912	-1.7451700496
H75	-1.2788896500	1.1780821693	-2.5029097848
H76	0.5815583446	-2.9878643981	-3.2610255062
H78	-0.3105886687	-3.3043010279	-1.7451700496
H80	-0.3808042613	-1.6965920102	-2.5029097848

***fac*-PhP** T_1 geometry:

atom	x	y	z
Ir1	0.0935730000	0.0103510000	0.3666140000
C2	-1.5227160000	-4.1022130000	2.5089740000
C3	-2.2199070000	-3.4870200000	1.4744700000
C4	-1.6805260000	-2.3273460000	0.9241320000
C5	-0.4798760000	-1.7402900000	1.3545740000
C6	0.1982040000	-2.4049670000	2.3819280000
C7	-0.3193500000	-3.5637140000	2.9592740000
H8	-1.9225860000	-5.0053870000	2.9610510000
H9	-3.1575440000	-3.8860720000	1.1034340000
H11	1.1345410000	-1.9957370000	2.7527960000
H12	0.2196480000	-4.0473290000	3.7703550000
C13	-2.6420080000	3.1948640000	2.8626830000
C14	-2.6475940000	1.8599670000	3.2854480000
C15	-1.9093050000	0.8981410000	2.6045770000
C16	-1.1209700000	1.2398440000	1.4953800000
C17	-1.1630710000	2.5996080000	1.0884090000
C18	-1.9015140000	3.5795430000	1.7521350000
H19	-3.2225240000	3.9383490000	3.4014420000
H20	-3.2305040000	1.5752080000	4.1578570000
H21	-1.9171270000	-0.1318110000	2.9503840000
H23	-1.8864900000	4.6032950000	1.3934400000
C24	4.2703990000	0.7327930000	2.7553030000
C25	3.1635720000	1.5040730000	3.1273360000
C26	1.9487930000	1.3591600000	2.4713930000

C27	1.7844620000	0.4210570000	1.4328410000
C28	2.9424390000	-0.3194470000	1.0806380000
C29	4.1709190000	-0.1898700000	1.7177280000
H30	5.2169650000	0.8517590000	3.2746400000
H31	3.2555750000	2.2165610000	3.9428690000
H32	1.0943730000	1.9519770000	2.7842660000
H34	5.0157600000	-0.7946140000	1.4064490000
C35	-1.6644840000	-0.5185550000	-0.6375840000
N33	-2.2977880000	-1.6330750000	-0.1453880000
N34	-2.4709980000	-0.0268410000	-1.6159410000
C45	1.4725470000	-1.2204520000	-0.5525620000
N36	1.4960530000	-2.2120160000	-1.4839920000
N37	2.7325100000	-1.2028480000	0.0065240000
C55	0.3290200000	1.8181940000	-0.5981860000
N39	0.9696120000	2.3566190000	-1.6866420000
N40	-0.4031710000	2.8681420000	-0.0564580000
C41	0.3685700000	-2.6428070000	-2.2768480000
C42	-2.2533870000	1.1813900000	-2.3821090000
C43	1.9217370000	1.6633910000	-2.5163560000
C56	2.7357790000	-2.8261540000	-1.5072280000
C57	3.5326110000	-2.1759730000	-0.5555990000
N46	4.7947780000	-2.4783680000	-0.2911400000
C59	5.2468200000	-3.5000490000	-1.0384600000
N48	4.5917400000	-4.1972710000	-1.9603150000
C61	3.3122380000	-3.8725300000	-2.2118970000
H65	6.2795170000	-3.7915540000	-0.8608850000
H67	2.7799290000	-4.4583400000	-2.9574050000
C62	-3.4971070000	-1.8342520000	-0.7922860000
C63	-3.6106100000	-0.8005850000	-1.7297920000
C64	-4.7607070000	-0.7666480000	-2.5046030000
N57	-5.6885460000	-1.7185440000	-2.3334960000
C66	-5.4618460000	-2.6570240000	-1.4158980000
N59	-4.4010180000	-2.7864090000	-0.6079400000
H70	-4.9598270000	0.0040570000	-3.2456570000
H72	-6.2357280000	-3.4130420000	-1.3037180000
C68	0.6671300000	3.6955430000	-1.8188510000
C69	-0.2151990000	4.0263690000	-0.7792640000
N66	-0.7397000000	5.2306340000	-0.5721600000
C71	-0.3176970000	6.1303200000	-1.4922290000
N68	0.5145800000	5.9490230000	-2.5018380000
C73	1.0415800000	4.7152830000	-2.6929840000
H77	-0.7190470000	7.1350760000	-1.3741840000
H79	1.7381900000	4.5805960000	-3.5151630000
H68	1.7481250000	1.9105030000	-3.5685110000
H69	2.9487550000	1.9381380000	-2.2528400000
H71	1.7922610000	0.5901110000	-2.3693580000
H73	-2.6737300000	1.0490360000	-3.3817920000
H74	-2.7291620000	2.0409790000	-1.9004100000
H75	-1.1834250000	1.3643670000	-2.4609730000
H76	0.7167880000	-2.9521110000	-3.2654050000
H78	-0.1514310000	-3.4780210000	-1.7969840000
H80	-0.3219500000	-1.8064270000	-2.3848250000

References

1 A. D. Bochevarov, E. Harder, T. F. Hughes, J. R. Greenwood, D. A. Braden, D. M. Philipp, D. Rinaldo, M. D. Halls, J. Zhang and R. A. Friesner, *Int. J. Quantum Chem.*, 2013, **113**, 2110–2142.

2 C. Adamo and V. Barone, *J. Chem. Phys.*, 1999, **110**, 6158–6170.

3 F. Neese, F. Wennmohs, U. Becker and C. Riplinger, *J. Chem. Phys.*, 2020, **152**, 224108.

4 K. Nozaki, *J. Chinese Chem. Soc.*, 2006, **53**, 101–112.

5 K. Mori, T. P. M. Goumans, E. van Lenthe and F. Wang, *Phys. Chem. Chem. Phys.*, 2014, **16**, 14523–14530.

6 C. F. R. Mackenzie, L. Zhang, D. B. Cordes, A. M. Z. Slawin, I. D. W. Samuel and E. Zysman-Colman, *Adv. Opt. Mater.*, 2023, **11**, 2201495.

7 C. Wu, K. Tong, M. Zhang, M. Ng, S. Zhang, W. Cai, S. Jung, Y. Wu, C. Yang, M. Tang and G. Wei, *Adv. Opt. Mater.*, 2022, **10**, 2200356..

8 Z.-L. Zhu, P. Gnanasekaran, J. Yan, Z. Zheng, C.-S. Lee, Y. Chi and X. Zhou, *Inorg. Chem.*, 2022, **61**, 8898–8908.

9 G. Sarada, A. Maheshwaran, W. Cho, T. Lee, S. H. Han, J. Y. Lee and S.-H. Jin, *Dye. Pigment.*, 2018, **150**, 1–8.

10 H. Li, Y.-M. Yin, H.-T. Cao, H.-Z. Sun, L. Wang, G.-G. Shan, D.-X. Zhu, Z.-M. Su and W.-F. Xie, *J. Organomet. Chem.*, 2014, **753**, 55–62.

11 H. Park, A. Maheshwaran, C. Moon, H. Lee, S. S. Reddy, V. G. Sree, J. Yoon, J. W. Kim, J. H. Kwon, J. Kim and S. Jin, *Adv. Mater.*, 2020, **32**, 2002120.

12 T. Sajoto, P. I. Djurovich, A. B. Tamayo, J. Oxgaard, W. A. Goddard and M. E. Thompson, *J. Am. Chem. Soc.*, 2009, **131**, 9813–9822.

13 J. Jin, Z. Zhu, J. Yan, X. Zhou, C. Cao, P.-T. Chou, Y.-X. Zhang, Z. Zheng, C.-S. Lee and Y. Chi, *Adv. Photonics Res.*, 2022, **3**, 2100381.

14 Y. Qin, X. Yang, J. Jin, D. Li, X. Zhou, Z. Zheng, Y. Sun, W. Y. Wong, Y. Chi and S. J. Su, *Adv. Opt. Mater.*, 2022, **10**, 1–13.